Fig. 3. Effect of nicotine on the expression of costimulatory/coinhibitory molecules on DCs. Expression of HLA-DR(A), CD40(A), CD80(B), CD86(B), PD-L1(C), PD-L2(C), ILT3(D) and ILT4 (D) on MoDCs or NiDCs stimulated with LPS (10 ng/ml) for 48 h was evaluated by FACS. Left panels: bar graphs are shown as mean values ± SD of five independent experiments. *$P < 0.05$ when compared with MoDCs stimulated with LPS. MFI: mean fluorescent intensity. Right panels: one representative FACS histogram of MoDCs (thin line) and NiDCs (thick line) of more than six independent experiments are shown.

tobacco toxicity that alters immune function. Considering the many components of cigarette smoke, nicotine may not be responsible for all types of tobacco toxicity. The expression of nicotinic acetylcholine receptors, however, indicates that the effects of nicotine may be transmitted and mediated by a specific cellular signaling pathway(s) coupled to immunological function. Although 10^{-3} M nicotine is greater than the pharmacological dose, the concentration of nicotine in saliva of smokers may reach mM levels in localized areas such as the oral cavity and respiratory tract [14–16]. We therefore assumed that direct and local exposure of high doses of nicotine to the inflammatory lesion with bleeding in gingival tissue initiates monocytes to differentiate into DC in inflamed gingival

microcirculation. In preliminary experiments, we used 10^{-8} to 10^{-2} M nicotine to investigate the effect of nicotine on DC phenotypic changes, and found that 10^{-3} M nicotine significantly induced DC characteristics. Additionally, we confirmed that 10^{-3} M nicotine did not impact DC viability. Therefore, we chose 10^{-3} M nicotine to induce differentiation of monocytes into DCs.

We report that *in vitro* differentiation of DCs from monocytes in the presence of nicotine yields a subset of DC (NiDCs) characterized by an altered phenotypic profile and modulated functions. CD1a is one of five members of the CD1 family and has been used as a DC biomarker [40]. There is however a significant heterogeneity in CD1a expression in DCs. Both CD1a (+ or −) DCs have been
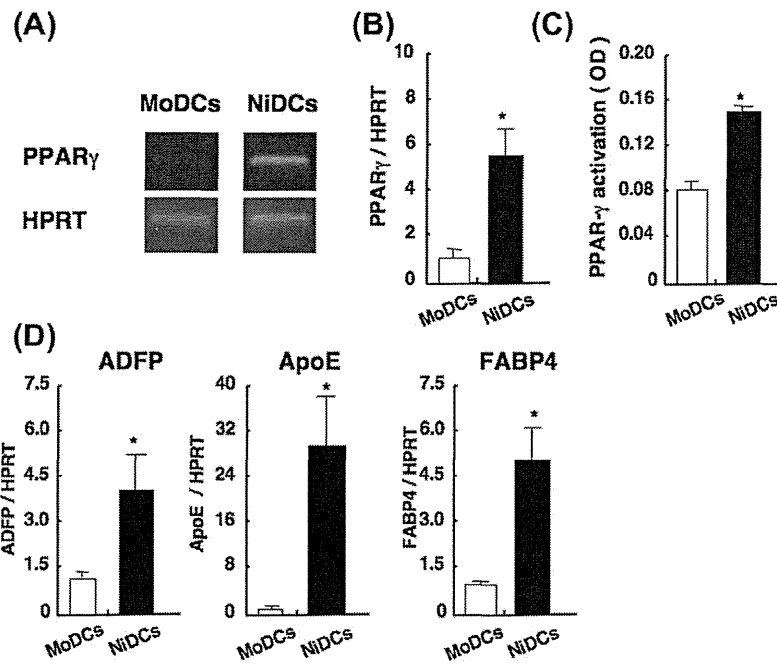
Fig. 4. Expression and activation of PPAR γ in MoDCs and NiDCs. (A) Representative RT-PCR analysis of PPAR γ mRNA expression. One representative profile of six performed. (B) Quantitative analyses of PPAR γ mRNA expression by real-time RT-PCR. mRNA levels are expressed as fold change above control mRNA (HPRT). Results are shown as mean values ± SD of five independent experiments. (C) Activation of PPAR γ in MoDCs and NiDCs. Nuclear extracts taken at a half-hour were analyzed by the TransAM PPAR γ assay. Results are shown as mean values ± SD of five independent experiments and are expressed as ratio of OD$_{450}$. (D) Expression of the PPAR γ target genes in MoDCs and NiDCs. Results are shown as mean values ± SD of five independent experiments. *P < 0.05 when compared with MoDCs.
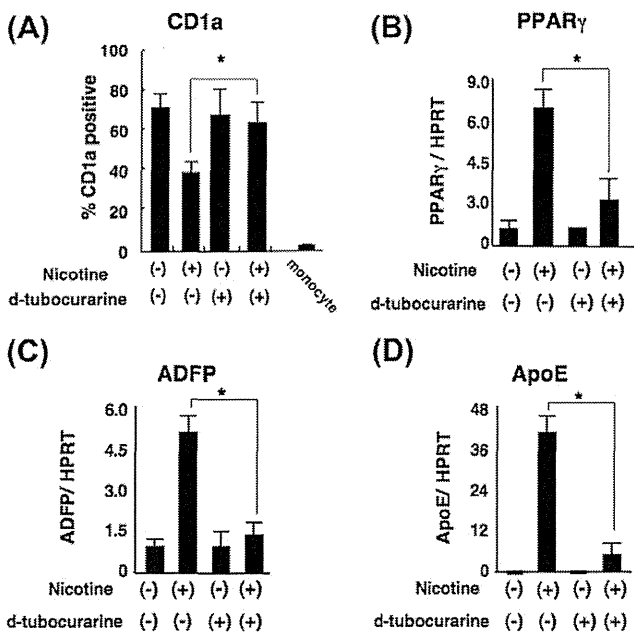

Fig. 5. Effect of d-tubocurarine, a non-selective nAChRs antagonist on mRNA expression of PPAR γ and PPAR γ target genes in MoDCs and NiDCs. (A) Expression of CD1a was examined at day 7 to evaluate the effect of nicotine and d-tubocurarine. Results are shown as mean values ± SD of five independent experiments. (B–D) Quantitative analyses of PPAR γ, ADFP, and ApoE mRNA expression by real-time RT-PCR. mRNA levels are expressed as fold change above control mRNA (HPRT). Results are shown as mean values ± SD of four independent experiments. *P < 0.05 when compared with DCs differentiated in the presence of nicotine with pretreatment of d-tubocurarine.

Fig. 6. Effect of d-tubocurarine, non-selective nAChRs antagonist on Th1 responses in MoDCs and NiDCs. (A) IL-12 (p40 + p70) production by MoDCs and NiDCs. MoDCs and NiDCs pretreated with d-tubocurarine (1 μM) were cultured in the presence of 10 ng/ml LPS for 48 h. Supernatants were then tested for IL-12 (p40 + p70) production by ELISA. (B) Supernatants of restimulated T cells were harvested and measured for IFN-γ level by ELISA. Results are shown as mean values ± SD of four independent experiments. *P < 0.05 when compared with NiDCs without pretreatment of d-tubocurarine.

identified in peripheral blood [41]. In addition, recent studies suggest that the ratio of +/− forms of CD1a DCs differentiated from monocytes can be altered depending on the culture conditions
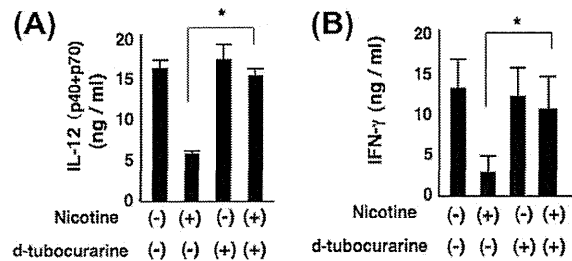
[42–45]. In our study, a significant reduction of CD1a+ expression is observed in NiDCs when compared with MoDCs. The effect of nicotine on decreasing CD1a expression is inhibited by pretreatment of cells with d-tubocurarine, a non-selective nAChR antagonist. These results indicate that nicotine interaction with nAChRs can mediate DC differentiation.

As seen in Fig. 1B, LPS-stimulated NiDC secreted lower amounts of pro-inflammatory cytokines such as IL-12 (p40 + p70) and TNF-α, compared with MoDCs. These data confirm results from previous studies in which nicotine and cigarette smoke extracts (CSE) suppressed DC function, impaired antigen-presentation to induce naive T cell proliferation and alter Th1 responses into those seen in Th2 cells [23,24]. These studies also described that CSE suppressed IL-12 production in activated DCs, and diminished the effects of costimulatory molecules such as CD40 and CD80. We observed poor induction of T cell proliferation by NiDCs, elevation of the coinhibitory molecules PD-L1 and ILT4, and a slight

upregulation of PD-L2 in LPS-stimulated NiDCs. Furthermore, ILT3 expression was maintained in NiDC after LPS-stimulation, although expression on LPS-stimulated MoDCs was reduced. Increased PD-L1 and PD-L2 expression combined with positive costimulatory molecules such as CD86 induce an immunotolerogenic function in DCs [46–48]. In addition, high expression of ILT3 and ILT4 on DCs is associated with immunotolerogenic characteristics [49,50]. The reduction in priming capacity of NiDCs may result from induction of inhibitory cell surface receptors.

PPAR γ has been reported to mediate several DC functions. PPAR γ-activated DCs altered the differentiation of naive CD4 T cells into Th2 cells [32,51]. In addition, PPAR-γ agonists inhibited TLR-mediated DC activation by interfering with the NF-κB and MAP kinase pathway [52]. In a conditional PPAR γ knockout mouse study, PPAR γ-activated DCs induced naive T cell anergy [31]. Other studies suggest that PPAR γ plays an important role in induction and maintenance of natural and induced Treg cells [53,54]. A recent report described that activation of PPAR γ strongly enhanced the expression of B7H1 (also termed PD-L1) [55]. We show that expression of PPAR-γ gene and PPAR-γ target genes are upregulated in NiDCs. ApoE plays important roles in lipoprotein clearance and homeostasis. ADRP plays a role in lipid body formation and cross-presentation of phagocytosed antigens to CD8⁺ T cells. FABP4 plays an important role in the regulation of insulin sensitivity. In addition, both ApoE and FABP4 deficiency lead to development of athelosclerosis. Among those molecules, ADRP is likely to have a role in DC antigen presenting function. However, there is no information at present that these genes are involved in T cell proliferation and differentiation. With regard to PPAR-γ expression in NiDCs, further studies are needed to investigate the possible role of nicotine in induction of Treg cells as our data suggests that nicotine may differentiate monocytes into tolerogenic DCs.

The molecular mechanism of elevated PPAR γ expression in NiDCs needs to be clarified. Results from recent studies indicate that α7nAChR is crucial to the regulation of systemic inflammation, and that nicotine and acetylcholine control inflammatory cytokine production from endotoxin-stimulated macrophages by inhibiting NF-κB pathway via α7nAChRs [11,13]. We demonstrate that pre-treatment of DCs with d-tubocurarine, a non-selective nAChR antagonist, reversed inhibition of CD1a expression, IL-12 production and Th1 responses in the presence of nicotine. One point that appears to be clear is that nicotine and nicotinic agonists prevent endotoxin-induced activation of the NF-κB pathway and induce expression of PPAR γ. Upregulation of PPAR γ and downregulation of NF-κB may synergistically induce the NiDC phenotype described previously. Blocking nAChRs by antagonist recovered Th1 response, however, there was no significant difference in IL-5 and IL-10 production between antagonist-treated NiDCs and control-NiDCs (data not shown). Presumably, the pathway inducing Th2 immune responses may be influenced by endocytosed nicotine, and not only by nicotine acting via nAChRs signaling.

Cigarette smoking leads to many health problems worldwide by significantly increasing the risk of diseases such as lung cancer, cardiovascular disease, COPD, rheumatoid arthritis and periodontal disease [1–5,56–58]. Smoking-related suppression of immune responses includes reduction of NK activity [59], and inhibition of microbicidal activity of macrophages [8,60]. Cigarette smoking and nicotine, however, may actually reduce severe inflammation in patients with ulcerative colitis (UC) [61,62]. In an animal study, conditional deletion of the PPAR γ-encoded gene in intestinal epithelial cells or macrophages caused an exacerbation of experimental colitis [30,53]. In addition, PPAR γ expression in the colonic mucosa is impaired in UC patients [63]. Results from these studies in addition to results from our study, indicate that nicotine signaling may induce expression and activation of PPAR γ.

In conclusion, our study provides new data indicating that nicotine reduces inflammatory cytokine production, and suppresses T cell priming capacity of DC via nAChRs. The suggested mechanism is nicotinic upregulation of coinhibitory molecules. The effect of nicotine may be mediated by PPAR γ expression. These studies suggest a link between the effects of nicotine on DC function and smoking-related diseases. Understanding the immuno-modulatory effects of nicotine will provide new and useful information for the prevention of smoking-related diseases.

References

[1] D. Carbone, Smoking and cancer, Am. J. Med. 93 (1992) 13S–17S.
[2] L. Erhardt, Cigarette smoking: an undertreated risk factor for cardiovascular disease, Atherosclerosis 205 (2009) 23–32.
[3] M.I. Ryder, The influence of smoking on host responses in periodontal infections, Periodontol 2000 (43) (2007) 267–277.
[4] G.G. Brusselle, G.F. Joos, K.R. Bracke, New insights into the immunology of chronic obstructive pulmonary disease, Lancet 378 (2011) 1015–1026.
[5] M.R. Stämpfli, G.P. Anderson, How cigarette smoke skews immune responses to promote infection, lung disease and cancer, Nat. Rev. Immunol. 9 (2009) 377–384.
[6] P.G. Holt, D. Keast, Environmentally induced changes in immunological function: acute and chronic effects of inhalation of tobacco smoke and other atmospheric contaminants in man and experimental animals, Bacteriol. Rev. 41 (1977) 205–216.
[7] Y. Geng, S.M. Savage, S. Razani-Boroujerdi, M.L. Sopori, Effects of nicotine on the immune response. II. Chronic nicotine treatment induces T cell anergy, J. Immunol. 156 (1996) 2384–2390.
[8] A.D. Maus, E.F. Pereira, P.I. Karachunski, R.M. Horton, D. Navaneetham, K. Macklin, W.S. Cortes, E.X. Albuquerque, B.M. Conti-Fine, Human and rodent bronchial epithelial cells express functional nicotinic acetylcholine receptors, Mol. Pharmacol. 54 (1998) 779–788.
[9] K. Kawashima, T. Fujii, Extraneuronal cholinergic system in lymphocytes, Pharmacol. Ther. 86 (2000) 29–48.
[10] H.S. Sekhon, Y. Jia, R. Raab, A. Kuryatov, J.F. Pankow, J.A. Whitsett, J. Lindstrom, E.R. Spindel, Prenatal nicotine increases pulmonary alpha7 nicotinic receptor expression and alters fetal lung development in monkeys, J. Clin. Invest. 103 (1999) 637–647.
[11] H. Wang, M. Yu, M. Ochani, C.A. Amella, M. Tanovic, S. Susarla, J.H. Li, H. Wang, H. Yang, L. Ulloa, Y. Al-Abed, C.J. Czura, K.J. Tracey, Nicotinic acetylcholine receptor alpha7 subunit is an essential regulator of inflammation, Nature 421 (2003) 384–388.
[12] M.R. Blanchet, A. Langlois, E. Israel-Assayag, M.J. Beaulieu, C. Ferland, M. Laviolette, Y. Cormier, Modulation of eosinophil activation in vitro by a nicotinic receptor agonist, J. Leukoc. Biol. 81 (2007) 1245–1251.
[13] H. Wang, H. Liao, M. Ochani, M. Justiniani, X. Lin, L. Yang, Y. Al-Abed, H. Wang, C. Metz, E.J. Miller, K.J. Tracey, L. Ulloa, Cholinergic agonists inhibit HMGB1 release and improve survival in experimental sepsis, Nat. Med. 10 (2004) 1216–1221.
[14] D. Hoffmann, J.D. Adams, Carcinogenic tobacco-specific N-nitrosamines in snuff and in the saliva of snuff dippers, Cancer Res. 41 (1981) 4305–4308.
[15] T. Sato, T. Abe, N. Nakamoto, Y. Tomaru, N. Koshikiya, J. Nojima, S. Kokabu, T. Sakata, A. Kobayashi, T. Yoda, Nicotine induces cell proliferation in association with cyclin D1 up-regulation and inhibits cell differentiation in association with p53 regulation in a murine pre-osteoblastic cell line, Biochem. Biophys. Res. Commun. 377 (2008) 126–130.
[16] C. Feyerabend, T. Higenbottam, M.A. Russell, Nicotine concentrations in urine and saliva of smokers and non-smokers, Br. Med. J. (Clin. Res. Ed.) 284 (1982) 1002–1004.
[17] J. Banchereau, R.M. Steinman, Dendritic cells and the control of immunity, Nature 392 (1998) 245–252.
[18] S. Akira, K. Takeda, T. Kaisho, Toll-like receptors: critical proteins linking innate and acquired immunity, Nat. Immunol. 2 (2001) 675–680.
[19] T.A. Wynn, T(H)-17: a giant step from T(H)1 and T(H)2, Nat. Immunol. 6 (2005) 1069–1070.
[20] K. Shortman, Y.J. Liu, Mouse and human dendritic cell subtypes, Nat. Rev. Immunol. 2 (2002) 151–161.

[21] Y. Belkaid, G. Oldenhove, Tuning microenvironments: induction of regulatory T cells by dendritic cells, Immunity 29 (2008) 362–371.

[22] M. Rimoldi, M. Chieppa, V. Salucci, F. Avogadri, A. Sonzogni, G.M. Sampietro, A. Nespoli, G. Viale, P. Allavena, M. Rescigno, Intestinal immune homeostasis is regulated by the crosstalk between epithelial cells and dendritic cells, Nat. Immunol. 6 (2005) 507–514.

[23] R. Vassallo, K. Tamada, J.S. Lau, P.R. Kroening, L. Chen, Cigarette smoke extract suppresses human dendritic cell function leading to preferential induction of Th-2 priming, J. Immunol. 175 (2005) 2684–2691.

[24] M. Nouri-Shirazi, E. Guinet, Evidence for the immunosuppressive role of nicotine on human dendritic cell functions, Immunology 109 (2003) 365–373.

[25] A. Aicher, C. Heeschen, M. Mohaupt, J.P. Cooke, A.M. Zeiher, S. Dimmeler, Nicotine strongly activates dendritic cell-mediated adaptive immunity: potential role for progression of atherosclerotic lesions, Circulation 107 (2003) 604–611.

[26] T.M. Willson, M.H. Lambert, S.A. Kliewer, Peroxisome proliferator-activated receptor gamma and metabolic disease, Annu. Rev. Biochem. 70 (2001) 341–367.

[27] F. Picard, J. Auwerx, PPAR(gamma) and glucose homeostasis, Annu. Rev. Nutr. 22 (2002) 167–197.

[28] C. Jiang, A.T. Ting, B. Seed, PPAR-gamma agonists inhibit production of monocyte inflammatory cytokines, Nature 391 (1998) 82–86.

[29] M. Ricote, A.C. Li, T.M. Willson, C.J. Kelly, C.K. Glass, The peroxisome proliferator-activated receptor-gamma is a negative regulator of macrophage activation, Nature 391 (1998) 79–82.

[30] J.I. Odegaard, R.R. Ricardo-Gonzalez, M.H. Goforth, C.R. Morel, V. Subramanian, L. Mukundan, A. Red Eagle, D. Vats, F. Brombacher, A.W. Ferrante, A. Chawla, Macrophage-specific PPARgamma controls alternative activation and improves insulin resistance, Nature 447 (2007) 1116–1120.

[31] L. Klotz, I. Dani, F. Edenhofer, L. Nolden, B. Evert, B. Paul, W. Kolanus, T. Klockgether, P. Knolle, L. Diehl, Peroxisome proliferator-activated receptor gamma control of dendritic cell function contributes to development of CD^{4+} T cell anergy, J. Immunol. 178 (2007) 2122–2131.

[32] P. Gosset, A.S. Charbonnier, P. Delerive, J. Fontaine, B. Staels, J. Pestel, A.B. Tonnel, F. Trottein, Peroxisome proliferator-activated receptor gamma activators affect the maturation of human monocyte-derived dendritic cells, Eur. J. Immunol. 31 (2001) 2857–2865.

[33] I. Szatmari, A. Pap, R. Ruhl, J.X. Ma, P.A. Illarionov, G.S. Besra, E. Rajnavolgyi, B. Dezso, L. Nagy, PPARgamma controls CD1d expression by turning on retinoic acid synthesis in developing human dendritic cells, J. Exp. Med. 203 (2006) 2351–2362.

[34] A. Nencioni, F. Grünebach, A. Zobywlaski, C. Denzlinger, W. Brugger, P. Brossart, Dendritic cell immunogenicity is regulated by peroxisome proliferator-activated receptor gamma, J. Immunol. 169 (2002) 1228–1235.

[35] M. Cernadas, J. Lu, G. Watts, M.B. Brenner, CD1a expression defines an interleukin-12 producing population of human dendritic cells, Clin. Exp. Immunol. 155 (2009) 523–533.

[36] P. Gogolak, B. Rethi, I. Szatmari, A. Lanyi, B. Dezso, L. Nagy, E. Rajnavolgyi, Differentiation of CD1a- and CD1a+ monocyte-derived dendritic cells is biased by lipid environment and PPARgamma, Blood 109 (2007) 643–652.

[37] P.R. Kroening, T.W. Barnes, L. Pease, A. Limper, H. Kita, R. Vassallo, Cigarette smoke-induced oxidative stress suppresses generation of dendritic cell IL-12 and IL-23 through ERK-dependent pathways, J. Immunol. 181 (2008) 1536–1547.

[38] E. Mortaz, Z. Lazar, L. Koenderman, A.D. Kraneveld, F.P. Nijkamp, G. Folkerts, Cigarette smoke attenuates the production of cytokines by human plasmacytoid dendritic cells and enhances the release of IL-8 in response to TLR-9 stimulation, Respir. Res. 10 (2009) 47.

[39] E. Mortaz, A.D. Kraneveld, J.J. Smit, M. Kool, B.N. Lambrecht, S.L. Kunkel, N.W. Lukacs, F.P. Nijkamp, G. Folkerts, Effect of cigarette smoke extract on dendritic cells and their impact on T-cell proliferation, PLoS ONE 4 (2009) e4946.

[40] M. Brigl, M.B. Brenner, CD1: antigen presentation and T cell function, Annu. Rev. Immunol. 22 (2004) 817–890.

[41] T. Ito, M. Inaba, K. Inaba, J. Toki, S. Sogo, T. Iguchi, Y. Adachi, K. Yamaguchi, R. Amakawa, J. Valladeau, S. Saeland, S. Fukuhara, S. Ikehara, A CD1a+/CD11c+ subset of human blood dendritic cells is a direct precursor of Langerhans cells, J. Immunol. 163 (1999) 1409–1419.

[42] C.Q. Xia, K.J. Kao, Heparin induces differentiation of CD1a+ dendritic cells from monocytes: phenotypic and functional characterization, J. Immunol. 168 (2002) 1131–1138.

[43] G. Castellano, A.M. Woltman, N. Schlagwein, W. Xu, F.P. Schena, M.R. Daha, C. van Kooten, Immune modulation of human dendritic cells by complement, Eur. J. Immunol. 37 (2007) 2803–2811.

[44] K. Laudanski, A. De, C. Miller-Graziano, Exogenous heat shock protein 27 uniquely blocks differentiation of monocytes to dendritic cells, Eur. J. Immunol. 37 (2007) 2812–2824.

[45] E.A. Laborde, S. Vanzulli, M. Beigier-Bompadre, M.A. Isturiz, R.A. Ruggiero, M.G. Fourcade, A.C. Catalan Pellet, S. Sozzani, M. Vulcano, Immune complexes inhibit differentiation, maturation, and function of human monocyte-derived dendritic cells, J. Immunol. 179 (2007) 673–681.

[46] A.H. Sharpe, E.J. Wherry, R. Ahmed, G.J. Freeman, The function of programmed cell death 1 and its ligands in regulating autoimmunity and infection, Nat. Immunol. 8 (2007) 239–245.

[47] C. Chen, Q.X. Qu, J.A. Huang, Y.B. Zhu, Y. Ge, Q. Wang, X.G. Zhang, Expression of programmed-death receptor ligands 1 and 2 may contribute to the poor stimulatory potential of murine immature dendritic cells, Immunobiology 212 (2007) 159–165.

[48] N. Selenko-Gebauer, O. Majdic, A. Szekeres, G. Hofler, E. Guthann, U. Korthauer, G. Zlabinger, P. Steinberger, W.F. Pickl, H. Stockinger, W. Knapp, J. Stockl, B7–H1 (programmed death-1 ligand) on dendritic cells is involved in the induction and maintenance of T cell anergy, J. Immunol. 170 (2003) 3637–3644.

[49] J.V. Ravetch, L.L. Lanier, Immune inhibitory receptors, Science 290 (2000) 84–89.

[50] C.C. Chang, R. Ciubotariu, J.S. Manavalan, J. Yuan, A.I. Colovai, F. Piazza, S. Lederman, M. Colonna, R. Cortesini, R. Dalla-Favera, N. Suciu-Foca, Tolerization of dendritic cells by T(S) cells: the crucial role of inhibitory receptors ILT3 and ILT4, Nat. Immunol. 3 (2002) 237–243.

[51] C. Faveeuw, S. Fougeray, V. Angeli, J. Fontaine, G. Chinetti, P. Gosset, P. Delerive, C. Maliszewski, M. Capron, B. Staels, M. Moser, F. Trottein, Peroxisome proliferator-activated receptor gamma activators inhibit interleukin-12 production in murine dendritic cells, FEBS Lett. 486 (2000) 261–266.

[52] S. Appel, V. Mirakaj, A. Bringmann, M.M. Weck, F. Grunebach, P. Brossart, PPAR-gamma agonists inhibit toll-like receptor-mediated activation of dendritic cells via the MAP kinase and NF-kappaB pathways, Blood 106 (2005) 3888–3894.

[53] R. Hontecillas, J. Bassaganya-Riera, Peroxisome proliferator-activated receptor gamma is required for regulatory CD^{4+} T cell-mediated protection against colitis, J. Immunol. 178 (2007) 2940–2949.

[54] E.A. Wohlfert, F.C. Nichols, E. Nevius, R.B. Clark, Peroxisome proliferator-activated receptor gamma (PPARgamma) and immunoregulation: enhancement of regulatory T cells through PPARgamma-dependent and -independent mechanisms, J. Immunol. 178 (2007) 4129–4135.

[55] L. Klotz, S. Hucke, D. Thimm, S. Classen, A. Gaarz, J. Schultze, F. Edenhofer, C. Kurts, T. Klockgether, A. Limmer, P. Knolle, S. Burgdorf, Increased antigen cross-presentation but impaired cross-priming after activation of peroxisome proliferator-activated receptor gamma is mediated by up-regulation of B7H1, J. Immunol. 183 (2009) 129–136.

[56] P.J. Barnes, Chronic obstructive pulmonary disease, N. Engl. J. Med. 343 (2000) 269–280.

[57] C. Heeschen, J.J. Jang, M. Weis, A. Pathak, S. Kaji, R.S. Hu, P.S. Tsao, F.L. Johnson, J.P. Cooke, Nicotine stimulates angiogenesis and promotes tumor growth and atherosclerosis, Nat. Med. 7 (2001) 833–839.

[58] K.G. Saag, J.R. Cerhan, S. Kolluri, K. Ohashi, G.W. Hunninghake, D.A. Schwartz, Cigarette smoking and rheumatoid arthritis severity, Ann. Rheum. Dis. 56 (1997) 463–469.

[59] M.F. Mian, N.M. Lauzon, M.R. Stampfli, K.L. Mossman, A.A. Ashkar, Impairment of human NK cell cytotoxic activity and cytokine release by cigarette smoke, J. Leukoc. Biol. 83 (2008) 774–784.

[60] T.E. King Jr., D. Savici, P.A. Campbell, Phagocytosis and killing of *Listeria monocytogenes* by alveolar macrophages: smokers versus nonsmokers, J. Infect. Dis. 158 (1988) 1309–1316.

[61] A.D. Harries, A. Baird, J. Rhodes, Non-smoking: a feature of ulcerative colitis, Br. Med. J. (Clin. Res. Ed.) 284 (1982) 706.

[62] B.M. Calkins, A meta-analysis of the role of smoking in inflammatory bowel disease, Dig. Dis. Sci. 34 (1989) 1841–1854.

[63] L. Dubuquoy, E.A. Jansson, S. Deeb, S. Rakotobe, M. Karoui, J.F. Colombel, J. Auwerx, S. Pettersson, P. Desreumaux, Impaired expression of peroxisome proliferator-activated receptor gamma in ulcerative colitis, Gastroenterology 124 (2003) 1265–1276.

Adiponectin regulates functions of gingival fibroblasts and periodontal ligament cells

T. Iwayama, M. Yanagita, K. Mori, K. Sawada, M. Ozasa, M. Kubota, K. Miki, Y. Kojima, M. Takedachi, M. Kitamura, Y. Shimabukuro, T. Hashikawa, S. Murakami
Division of Oral Biology and Disease Control, Department of Periodontology, Osaka University Graduate School of Dentistry, Yamadaoka, Suita, Osaka, Japan

Iwayama T, Yanagita M, Mori K, Sawada K, Ozasa M, Kubota M, Miki K, Kojima Y, Takedachi M, Kitamura M, Shimabukuro Y, Hashikawa T, Murakami S. Adiponectin regulates functions of gingival fibroblasts and periodontal ligament cells. J Periodont Res 2012; 47: 563–571. © 2012 John Wiley & Sons A/S

Background and Objective: Adiponectin is a cytokine constitutively produced by adipocytes and exhibits multiple biological functions by targeting various cell types. However, the effects of adiponectin on primary gingival fibroblasts and periodontal ligament cells are still unexplored. Therefore, we investigated the effects of adiponectin on gingival fibroblasts and periodontal ligament cells.

Material and Methods: The expression of adiponectin receptors (AdipoR1 and AdipoR2) on human gingival fibroblasts (HGFs), mouse gingival fibroblasts (MGFs) and human periodontal ligament (HPDL) cells was examined using RT-PCR and western blotting. HGFs and MGFs were stimulated with interleukin (IL)-1β in the presence or absence of adiponectin, and the expression of IL-6 and IL-8 at both mRNA and protein levels was measured by real-time PCR and ELISA, respectively. Furthermore, small interfering RNAs (siRNAs) in MGFs were used to knock down the expression of mouse AdipoR1 and AdipoR2. The effects of adiponectin on the expression of alkaline phosphatase (*ALP*) and runt-related transcription factor 2 (*Runx2*) genes were evaluated by real-time PCR. Mineralized nodule formation of adiponectin-treated HPDL cells was revealed by Alizarin Red staining.

Results: AdipoR1 and AdipoR2 were expressed constitutively in HGFs, MGFs and HPDL cells. Adiponectin decreased the expression of IL-6 and IL-8 in IL-1β-stimulated HGFs and MGFs. AdipoR1 siRNA in MGFs revealed that the effect of adiponectin on reduction of IL-6 expression was potentially mediated via AdipoR1. Adiponectin-treated HPDL cells promoted the expression of *ALP* and *Runx2* mRNAs and up-regulated ALP activity. Furthermore, adiponectin enhanced mineralized nodule formation of HPDL cells.

Conclusion: Our observations demonstrate that adiponectin exerts anti-inflammatory effects on HGFs and MGFs, and promotes the activities of osteoblasto-genesis of HPDL cells. We conclude that adiponectin has potent beneficial functions to maintain the homeostasis of periodontal health, improve periodontal lesions, and contribute to wound healing and tissue regeneration.

Shinya Murakami, PhD, DDS, Division of Oral Biology and Disease Control, Department of Periodontology, Osaka University Graduate School of Dentistry, Yamadaoka 1-8, Suita, Osaka 565-0871, Japan
Tel: +81 6 6879 2930
Fax: +81 6 6879 2934
e-mail: ipshinya@dent.osaka-u.ac.jp

Periodontal disease is a chronic inflammatory disease initiated by the biofilm of periodontopathic bacteria, leading to the destruction of peri-odontal tissues. Periodontal disease can be exacerbated by many factors;

for example, systemic diseases, such as diabetes, osteoporosis and immunodeficiency diseases, have been shown to result in an increased risk for periodontal disease (1). Interestingly, recent epidemiologic studies have suggested that obesity is also a risk factor for periodontitis (2,3). Obesity, which induces insulin resistance following systemic chronic inflammation (4), is one of the leading causes of type 2 diabetes, which is closely associated with periodontal diseases. Thus, it is possible that obesity and metabolic syndrome could be risk factors for the progression of periodontal diseases; however, the precise mechanism of how obesity results in the destruction of periodontal tissue remains unclear.

Adipokines, secreted by adipose tissue, can influence insulin resistance, inflammation and the cardiovascular system (5). Adiponectin – an adipokine – circulates in high concentrations in plasma (6). Two adiponectin receptors (AdipoRs) have been reported to be expressed on various tissues and cells (7). Importantly, hypo-adiponectinemia has been observed in patients with type 2 diabetes mellitus, obesity and coronary artery disease (8,9). Physiological concentrations of adiponectin suppressed tumor necrosis factor-α-induced inflammatory responses in human endothelial cells and macrophages (10). Recent studies have revealed that the concentrations of adiponectin in serum of patients with severe periodontitis are lower than those in serum from healthy subjects (11,12). Periodontal treatment has also been shown to increase the levels of adiponectin in chronic periodontitis (13). Interestingly, Yamaguchi *et al.* (14) reported that the levels of expression of AdipoRs were decreased in sites of severe periodontitis. These data suggest that adiponectin is involved in the homeostasis of periodontal tissues and may modulate inflammatory responses at periodontal lesions.

In recent years, adiponectin and AdipoRs have been reported to be expressed in osteoblasts (15,16), suggesting that adiponectin may be involved not only in anti-inflammatory functions but also in bone metabolism. Among periodontal tissues, periodon-

tal ligament (PDL) cells have the potential to regulate neogenesis of alveolar bone and cementum and play important roles in events of wound healing and regeneration following periodontal tissue breakdown caused by progression of periodontal diseases. Considering the multifunctional role of adiponectin, adiponectin may affect the functional characteristics of PDL cells, which can differentiate into mineralized tissue-forming cells such as osteoblasts and cementoblasts (17).

In this study we investigated the anti-inflammatory effect of adiponectin on human gingival fibroblasts (HGFs) and mouse gingival fibroblasts (MGFs). In addition, we examined the physiological effect of adiponectin on cytodifferentiation of human PDL (HPDL) cells. The results showed that adiponectin suppressed proinflammatory cytokines induced by interleukin (IL)-1β stimulation, possibly via AdipoR1. Furthermore, adiponectin promoted the differentiation and mineralization of HPDL cells.

Material and methods

Reagents

Recombinant human and mouse IL-1β, adiponectin and normal rabbit IgG were obtained from R&D Systems (Minneapolis, MN, USA). Anti-adipoR1 IgG was obtained from Santa Cruz Biotechnology (Santa Cruz, CA, USA) and Alpha Diagnostic Intl. Inc. (San Antonio, TX, USA).

Cells

Before participating in this study, all human subjects provided informed consent according to a protocol that was reviewed and approved by the Institutional Review Board of the Osaka University Graduate School of Dentistry. HGFs were obtained from biopsies of healthy gingiva taken from healthy volunteers, as previously described (18). HGFs were used for experiments at passages 4–10. MGFs were isolated from healthy gingival tissue of the first premolar teeth of BALB/c mice. When the cells that grew out from the explants reached

confluence, they were separated by treatment with 0.53 mM EDTA containing 0.05% trypsin, collected by centrifugation and cultured on plastic culture dishes containing standard medium (standard medium is α-minimal essential medium containing 10% fetal calf serum) until they reached confluence. After 12 passages, the clonal MGF cell line was established using the limiting-dilution method. HPDL cells were isolated and maintained as described previously (19,20). For the induction of cytodifferentiation, HPDL cells were cultured in α-minimal essential medium (α-MEM) containing 10% fetal calf serum, 10 mM β-glycerophosphate and 50 μg/mL of ascorbic acid [(calcification-inducing medium (C-Med)]. C-Med was replaced every 3 d.

RT-PCR

Total RNA was isolated from HGFs, HPDL cells and MGFs using an RNA-Bee kit (TEL-TEST, Inc., Friendswood, TX, USA) according to the manufacturer's instructions. cDNA was synthesized and amplified using PCR, as described previously (18). Oligonucleotide PCR primers specific for adiponectin and AdipoRs were synthesized by Clontech (Palo Alto, CA, USA). The sequences of the primers are shown in Table 1. Hypoxanthine phosphoribosyltransferase (HPRT) and glyceraldehyde-3-phosphate dehydrogenase (GAPDH) served as housekeeping genes.

Western blot analysis

HGFs, HPDL cells and MGFs were lysed in RIPA buffer [25 mM Tris–HCl, pH 7.6, 150 mM NaCl, 1% Nonidet P-40 (NP-40), 1% sodium deoxycholate, 0.1% SDS, 10 mM Na$_3$VO$_4$ and 10 μg/mL each of aprotinin and leupeptin]. The proteins were separated by SDS-PAGE and transferred to nitrocellulose membranes. The membranes were incubated with 10% bovine serum albumin for 1 h and subsequently with rabbit polyclonal anti-adiponectin Ig (Alpha Diagnostic International inc.) or goat polyclonal anti-AdipoR Ig (Santa Cruz Biotechnology) for 1 h at

Table 1. Primers used for RT-PCR

Gene		Sequence	
Human	Forward	5'-CGA GAT GTG ATG AAG GAG ATG GG-3'	304 bp
HPRT1	Reverse	5'-GCC TGA CCA AGG AAA GCA AAG TC-3'	
Human	Forward	5'-CAA ACA GCC CCA AAG TCA AT-3'	288 bp
Adiponectin	Reverse	5'-TCT CAG GTG AGG TGG GAA AC-3'	
Human	Forward	5'-AAA CTG GCA ACA TCT GGA CC-3'	300 bp
AdipoR1	Reverse	5'-GCT GTG GGG AGC AGT AGA AG-3'	
Human	Forward	5'-ACA GGC AAC ATT GGA CA CA-3'	267 bp
AdipoR2	Reverse	5'-CCA AGG AAC AAA ACT TCC CA-3'	
Mouse	Forward	5'-AGG TTG TCT CCT GCG ACT TC-3'	211 bp
GAPDH	Reverse	5'-CTT GCT CAG TGT CCT TGC TG-3'	
Mouse	Forward	5'-ATC TGA CGA CAC CAA AGG-3'	226 bp
Adiponectin	Reverse	5'-TCT CCA GGA GTG CCA TCT CT-3'	
Mouse	Forward	5'-TGC CCT CCT TTC GGG CTT GC-3'	529 bp
AdipoR1	Reverse	5'-GCC TTG ACA AAG CCC TCA GCG ATA G-3'	
Mouse	Forward	5'-TCT TCC TGT GCC TGG GGA TCT T-3'	254 bp
AdipoR2	Reverse	5'-CCC GAT ACT GAG GGG TGG CAA A-3'	

AdipoR1, adiponectin receptor 1; *AdipoR2*, adiponectin receptor 2; *GAPDH*, glyceraldehyde-3-phosphate dehydrogenase; *HPRT1*, hypoxanthine phosphoribosyltransferase-1.

Real-time PCR

HGFs and MGFs were seeded in a six-well plate at a density of 3×10^5 cells and 1.2×10^6 cells/well, respectively. Cells were grown to confluence in standard medium. Following 18 h of preincubation in the presence or absence of adiponectin, cells were treated with or without 0.1 ng/mL of IL-1β, then total RNA was isolated and precipitated. cDNA was synthesized and mixed with SYBR Green PCR Master Mix (Applied Biosystems, Foster City, CA) and gene-specific primers (Takara Bio, Shiga, Japan). Real-time PCR was performed using a 7300 Fast Real-Time PCR System (Applied Biosystems). The sequences of the primers are shown in Table 2. HPRT and GAPDH served as housekeeping genes.

Measurement of inflammatory cytokines in culture supernatants

HGFs and MGFs were seeded in a 12-well plate at a density of 1.8×10^5 and 7.2×10^5 cells, respectively, and grown to confluence in standard medium. Following 18 h of preincubation

with or without adiponectin, cells were treated with or without 0.5 ng/mL of IL-1β. In some experiments, cells were pretreated for 1 h with anti-adiponectin Ig. At the end of the incubation periods, the supernatants were collected and the levels of IL-6 and IL-8 (HGFs only) protein were measured using ELISA kits (R&D Systems) according to the manufacturer's instructions.

RNA interference

Small interfering RNA (siRNA) was used to knock down the expression of mouse AdipoR1 and AdipoR2. The AdipoR1 and AdipoR2 siRNAs, and a

negative-control siRNA (Silencer Select Negative Control #1 siRNA), were synthesized by Applied Biosystems. Silencer 1 Negative Control #1 siRNA was designed to have no significant sequence similarity to mouse, rat or human transcript sequences. MGFs were placed on a six-well culture dish. Twenty-four hours after incubation, MGFs, at 40–50% confluence, were transfected with siRNA AdipoR1, siRNA AdipoR2 or negative-control siRNA. The cells were transfected with 200 pmol of siRNA and negative-control siRNA using Lipofectamine 2000 (Invitrogen Corp, Carlsbad, CA, USA) according to the

Table 2. Primers used for real-time PCR

Gene		Sequence	
Human	Forward	5'-GGC AGT ATA ATC CAA AGA TGG TCA A-3'
HPRT1	Reverse	5'-GTC AAG GGC ATA TCC TAC AAC AAA C-3'
Human	Forward	5'-AAG CCA GAG CTG TGC AGA TGA GTA-3'
IL6	Reverse	5'-TGT CCT GCA GCC ACT GGT TC-3'
Human	Forward	5'-ACA CTG CGC CAA CAC AGA AAT TA-3'
IL8	Reverse	5'-TTT GCT TGA AGT TTC ACT GGC ATC-3'
Human	Forward	5'-GGA CCA TTC CCA CGT CTT CAC-3'
ALP	Reverse	5'-CCT TGT AGC CAG GCC CAT TG-3'
Human	Forward	5'-CAC TGG CGC TGC AAC AAG A-3'
RUNX2	Reverse	5'-CAT TCC GGA GCT CAG CAG AAT AA-3'
Mouse	Forward	5'-TGT GTC CGT CGT GGA TCT GA-3'
GAPDH	Reverse	5'-TTG CTG TTG AAG TCG CAG GAG-3'
Mouse	Forward	5'-CCA CTT CAC AAG TCG GAG GCT TA-3'
IL6	Reverse	5'-GCA AGT GCA TCA TCG TTG TTC ATA C-3'

ALP, alkaline phosphatase; *GAPDH*, glyceraldehyde-3-phosphate dehydrogenase; *HPRT1*, hypoxanthine phosphoribosyltransferase-1; *IL6*, interleukin-6; *IL8*, interleukin-8; *RUNX2*, runt-related transcription factor 2.

manufacturer's instructions. The cells were then analyzed using real-time PCR.

Determination of alkaline phosphatase activity, and staining with Alizarin Red

Alkaline phosphatase (ALP) activity was assessed according to the procedure described previously (20,21). Histochemical analysis of calcified nodules was performed using the Alizarin Red staining method (20,22). The density of calcified nodules in each well was calculated using the WinRoof software program (Mitani Corporation, Fukui, Japan).

Statistical analysis

The results were analyzed for statistical significance using the Student's *t*-test. Differences were considered significant at $p < 0.05$.

Results

Expression of AdipoR1 and AdipoR2, but not adiponectin, was detected in HGFs, HPDL cells and MGFs

To examine the expression of adiponectin and its receptors (AdipoR1 and AdipoR2) and mRNA and protein in HGFs, HPDL cells and MGFs, we performed RT-PCR amplification and western blotting. As shown in Fig. 1A and 1B, mRNA transcripts and protein for AdipoR1 and AdipoR2, but not for adiponectin, were detected in all cell types investigated.

Adiponectin reduced the expression of proinflammatory cytokines in IL-1β-stimulated HGFs

To the effect of adiponectin on the expression of proinflammatory cytokines in IL-1β-stimulated HGFs, HGFs were pretreated with adiponectin for 18 h before 2.5 h of stimulation with IL-1β, whereupon real-time PCR was performed. As shown in Fig. 2A, adiponectin significantly reduced the expression of *IL6* and *IL8* mRNAs. For assessment of IL-6 and IL-8 pro-
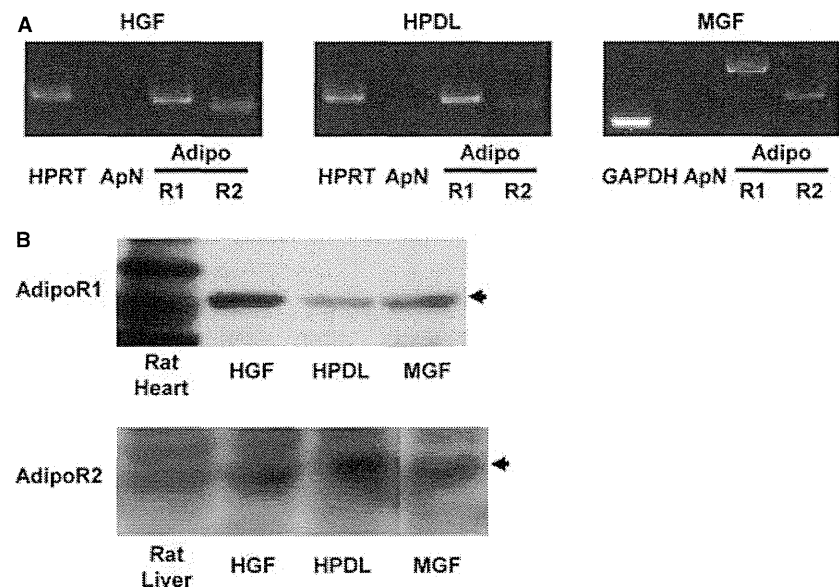
duction, adiponectin-pretreated HGFs were stimulated with 0.5 ng/mL of IL-1β, harvested after 12 h and then assayed using ELISA. Adiponectin also reduced the production of IL-6 protein and IL-8 protein (Fig. 2B).

AdipoR1 knockdown abrogated the adiponectin-induced reduction of IL-6 expression in MGFs

To examine the effect of adiponectin on the expression of IL-6 in IL-1β-stimulated MGFs, MGFs were pretreated with adiponectin for 18 h before stimulation with IL-1β for 2.5 h, whereupon real-time PCR was performed. As shown in Fig. 3A, adiponectin significantly reduced the expression of *IL6* mRNA. To assess the production of IL-6 protein, adiponectin-pretreated MGF were stimulated with 0.5 ng/mL of IL-1β, harvested after 12 h and then assayed using ELISA. Adiponectin also reduced the production of IL-6 protein (Fig. 3B). To elucidate the effect of adiponectin via AdipoRs, siRNA was used to block the expression of *AdipoR1* and *AdipoR2* mRNAs. As shown

in Fig. 4A and 4B, real-time PCR revealed that treatment with siRNA-AdipoR1 and siRNA-AdipoR2 significantly reduced the expression of AdipoR1 and AdipoR2 in MGFs compared with negative-control siRNA (Fig. 4A and 4B). Whereas IL-1β-induced expression of IL-6 in MGF treated with negative-control siRNA was significantly suppressed by adiponectin treatment, these suppressive effects were attenuated in MGFs treated with siRNA for AdipoR1 (Fig. 4C). By contrast, treatment with siRNA for AdipoR2 did not suppress IL-1β-induced expression of IL-6 by adiponectin (Fig. 4D). These results suggest that adiponectin reduces IL-6 expression in MGFs possibly via AdipoR1.

Anti-AdipoR1 Ig attenuated the adiponectin-induced reduction of IL-6 expression in HGF

To elucidate the effect of adiponectin via AdipoR1, HGFs were pretreated with control antibodies or with two types of anti-AdipoR1 polyclonal Igs and then stimulated with IL-1β in the presence or absence of adiponectin.
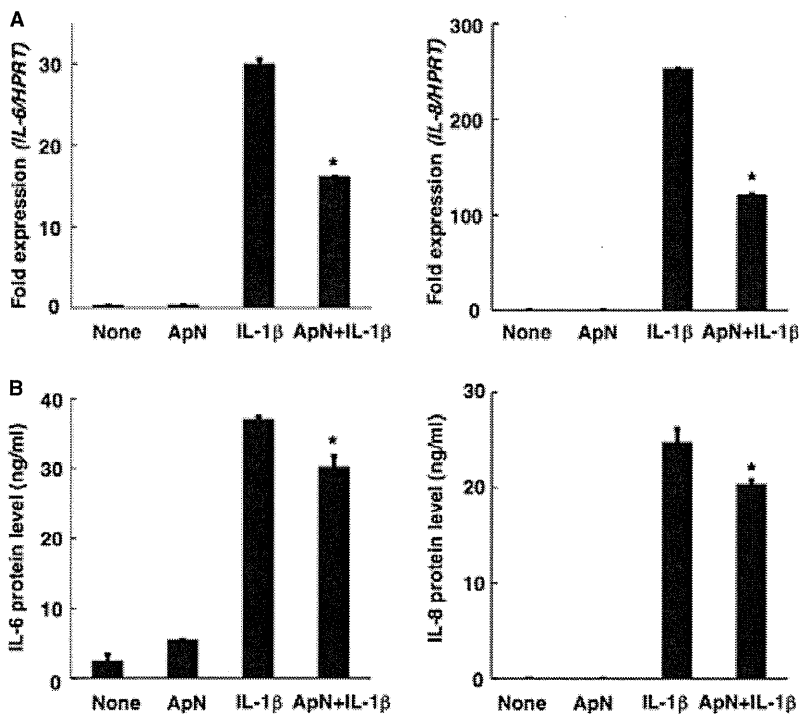

Fig. 1. Expression of adiponectin (ApN), adiponectin receptor 1 (AdipoR1) and adiponectin receptor 2 (AdipoR2). (A) Expression of *ApN*, *AdipoR1* and *AdipoR2* genes in human gingival fibroblasts (HGFs), human periodontal ligament (HPDL) cells and mouse gingival fibroblasts (MGFs) was examined by RT-PCR. (B) Expression of AdipoR1 and AdipoR2 proteins in HGFs, HPDL cells and MGFs was detected using western blotting. The data represent one of three independent experiments. GAPDH, glyceraldehyde-3-phosphate dehydrogenase; HPRT, hypoxanthine phosphoribosyltransferase.

A

B

Fig. 2. Adiponectin reduced interleukin (IL)-1β-induced production of IL-6 and IL-8 in human gingival fibroblasts (HGFs). (A) Expression of *IL6* and *IL8* genes in HGFs was examined using real-time PCR. HGFs were pretreated with adiponectin (ApN; 5 µg/mL) for 18 h, stimulated with IL-1β (0.1 ng/mL) for 2.5 h and then total RNA was isolated. (B) The levels of IL-6 and IL-8 protein in HGF cultured condition medium were measured using ELISA. HGFs were pretreated with adiponectin (ApN; 10 µg/mL) for 18 h and stimulated for 12 h with IL-1β (0.5 ng/mL). Data are the mean ± standard deviation of triplicate determinations. *p < 0.05 compared with IL-1β-stimulated HGF without ApN pretreatment. HPRT, hypoxanthine phosphoribosyltransferase.

A

B

Fig. 3. Adiponectin reduced interleukin (IL)-1β-induced expression of IL-6 in mouse gingival fibroblasts (MGFs). (A) Expression of the *IL6* gene in MGFs was examined by real-time PCR. MGFs were pretreated with adiponectin (ApN; 20 µg/mL) for 18 h, stimulated with IL-1β (0.5 ng/mL) for 2.5 h and then total RNA was isolated. (B) The level of IL-6 protein in MGF cultured condition medium was measured by ELISA. MGFs were pretreated with adiponectin (ApN; 20 µg/mL) for 18 h and stimulated with IL-1β (0.5 ng/mL) for 12 h. Data are the mean ± standard deviation of triplicate determinations. *p < 0.05 compared with IL-1β-stimulated MGFs without pretreatment of adiponectin. GAPDH, glyceraldehyde-3-phosphate dehydrogenase.

After 12 h, IL-6 production in the culture supernatants was assayed using ELISA. As shown in Fig. 5, anti-AdipoR1 Igs significantly attenuated the suppression of IL-1β-induced IL-6 expression by adiponectin. These results suggest that adiponectin reduces IL-6 expression in the IL-1β-stimulated HGFs possibly via AdipoR1.

Adiponectin promoted the differentiation and mineralization of HPDL cells

Next, we examined whether or not adiponectin would promote the differentiation and mineralization of HPDL cells. As shown in Fig. 6A, ALP activity in HPDL cells was significantly enhanced in the presence of adiponectin. Real-time PCR revealed that adiponectin significantly enhanced the expression of *ALP* and runt-related transcription factor 2 (*Runx2*; an

important transcription factor involved in osteoblastic differentiation and mineralization) (23) genes in HPDL cells cultured with C-Med in the presence of adiponectin (Fig. 6B and 6C) compared with C-Med only. Subsequently, mineralized nodule formation by HPDL cells on day 18 was investigated. As shown in Fig. 7A and 7B, adiponectin significantly increased the intensity of Alizarin Red staining. These results suggest that adiponectin promotes the differentiation and mineralization of HPDL cells.

Discussion

Adiponectin is an abundant serum protein, with concentrations in the order of 3–30 µg/mL (10). In this study, we demonstrated, for the first time, that physiological concentrations of adiponectin suppress IL-1β-induced IL-6 and IL-8 expression in HGFs, and IL-6 in
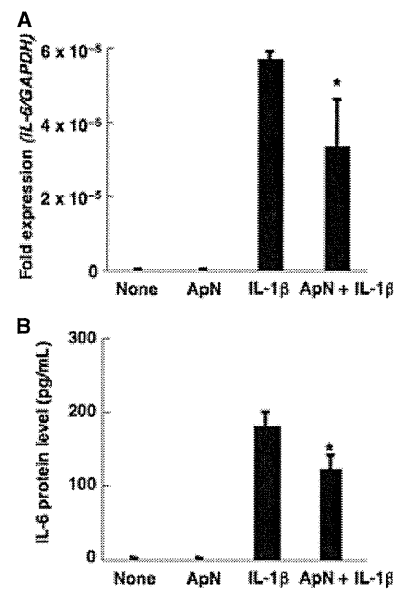
MGFs, at mRNA and protein levels, possibly via AdipoR1 signaling. We also showed that adiponectin enhances the differentiation and mineralization of HPDL cells. Unfortunately, however, mouse IL-8 has not yet been identified. As mouse CXCL1 is known to be the functional homolog of human IL-8, we examined the expression CXCL1 in preliminary studies (data not shown). In these studies, we found that adiponectin significantly reduced the expression of *CXCL1* mRNA. However, the expression of CXCL1 protein was not reduced by adiponectin (data not shown).

Several previous studies have reported that adiponectin is the immunomodulatory cytokine for the function of monocytes, macrophages and
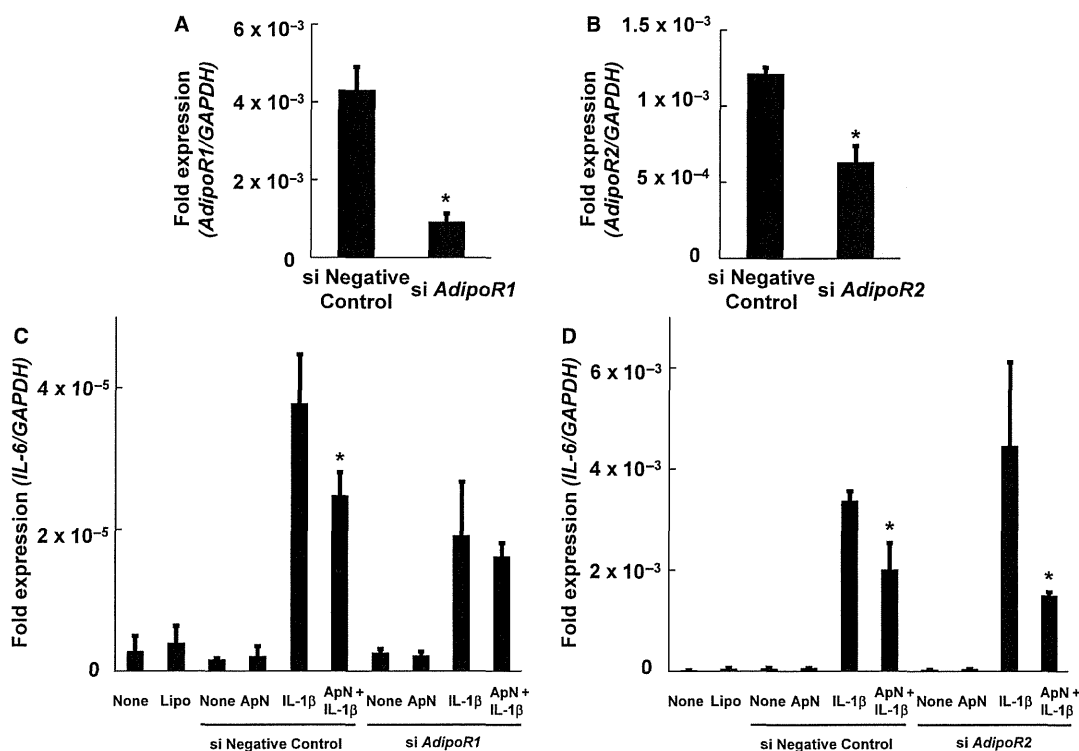
Fig. 4. Silencing adiponectin receptor 1 (AdipoR1) using small interfering (si)RNA attenuated the suppression of interleukin-6 (*IL6*) gene expression in mouse gingival fibroblasts (MGFs) stimulated with IL-1β. (A and B) MGFs transfected with AdipoR1, AdipoR2, or negative-control siRNAs were cultured for 24 h. *AdipoR1* and *AdipoR2* mRNAs were quantified using real-time PCR. These data represent one of three independent experiments. Data are the mean ± standard deviation of triplicate determinations (*p < 0.05). (C and D) Expression of the *IL6* gene in MGFs was examined using real-time PCR. MGFs transfected with AdipoR1, AdipoR2, or negative-control siRNAs were cultured for 24 h. The cells were seeded, pretreated with adiponectin (ApN; 20 µg/mL) for 18 h, stimulated with IL-1β (0.5 ng/mL) for 2 h and then total RNA was isolated. Data are the mean ± standard deviation of triplicate determinations. *p < 0.05 compared with IL-1β-stimulated MGFs without ApN pretreatment. GAPDH, glyceraldehyde-3-phosphate dehydrogenase; Lipo, lipofectamine 2000.

endothelial cells (10) and exhibits functional activity through binding to two AdipoRs. A recent systematic review concluded that there was a positive association between periodontal disease and obesity across diverse populations (3). The plasma adiponectin level in obese individuals was decreased compared with that in non-obese individuals (24). Saito *et al.* (11) previously reported that serum adiponectin levels in women with periodontitis were lower than in those with healthy gingiva, although this difference was not significant. Additionally, Yamaguchi *et al.* (14) revealed that the expression levels of AdipoRs in regions of periodontal disease were lower than in healthy gingival tissue. In mice with collagen-induced arthritis, adiponectin mitigated the severity of diseases (25). In addition, adiponectin suppressed the expression of inflammatory cytokines in stimulated rheumatoid arthritis

synovial fibroblasts (25). We found that HGFs, HPDL cells and MGFs expressed AdipoR1 and AdipoR2, but not adiponectin (Fig. 1). Additionally, we showed that suppression of AdipoR1 expression by its siRNA and anti-AdipoR1 Ig abrogated the anti-inflammatory actions of the cells, suggesting that adiponectin promoted these responses through the action of AdipoR1, at least in part on gingival fibroblasts (Figs 4 and 5).

Recent studies have demonstrated that AdipoRs are also expressed on osteoblasts (15,16,26). In the present study we showed that AdipoR1 and AdipoR2 expressed on HPDL cells and adiponectin enhanced ALP activity, expression of *ALP* and *Runx2* genes, and mineralized nodule formation in HPDL cells (Figs 6 and 7). ALP is an enzyme marker of osteoblasts and participates in mineralization (27). Runx2 has been identified as an important transcription

factor that is involved in bone formation and osteoblast differentiation (23). Thus, enhanced expression of *ALP* and *Runx2* genes, stimulated by adiponectin, were correlated with the mineralization of HPDL cells. In this study we did not directly examine the possible involvement of AdipoR1 in differentiation and mineralization of HPDL cells. However, a recent study reporting that adiponectin induced the differentiation and mineralization of osteoblastic MC3T3-E1 via AdipoR1 (26) suggests that the adiponectin–AdipoR1 pathway is also involved in the cytodifferentiation of HPDL cells. Although the functional roles of adiponectin in periodontal tissues have not been fully clarified, adiponectin should be involved in maintaining the homeostasis of periodontal tissue.

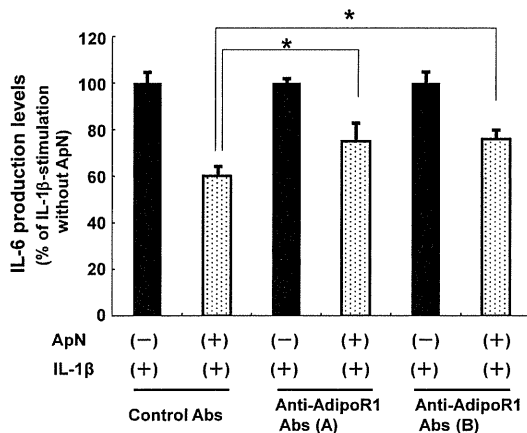In this study, we demonstrated two functional aspects of adiponectin: the

Fig. 5. Anti-adiponectin receptor 1 (AdipoR1) Igs attenuated the suppression of interleukin (IL)-6 production in human gingival fibroblasts (HGFs) stimulated with IL-1β. Cells were pretreated with control antibodies or with anti-AdipoR1 Igs for 1 h, incubated with adiponectin (ApN; 10 μg/mL) for 18 h and then stimulated with IL-1β (0.5 ng/mL) for 12 h. The levels of IL-6 protein in HGF cultured condition medium were measured using ELISA. Data are the mean ± standard deviation of triplicate determinations. Normalized data are shown as a percentage of the value in HGFs pretreated with the respective antibodies in the absence of ApN. *p < 0.05 compared with control antibody-pretreated HGFs in the presence of ApN.

first was an anti-inflammatory effect on gingival fibroblasts and the second was enhancement of cytodifferentiation in HPDL cells. Although we did not perform studies to clarify the signal pathway initiated following the activation of AdipoR1, accumulating evidence suggests that adiponectin increases the activities of sirtuin1 (SIRT1) and adenosine monophosphate-activated protein kinase (AMPK; 10). SIRT1 is an NAD^+-dependent deacetylase that interacts with and deacetylates p65 of nuclear factor-κB and subsequently inhibits the expression of inflammatory genes (28). Adiponectin has been shown to increase the levels of SIRT1 protein and to suppress lipopolysaccharide (LPS)-stimulated tumor necrosis factor-α production in Kupffer cells (29). AMPK is a heterotrimeric serine kinase responsive to a variety of cellular stimuli. In osteoblastic cells, AMPK is
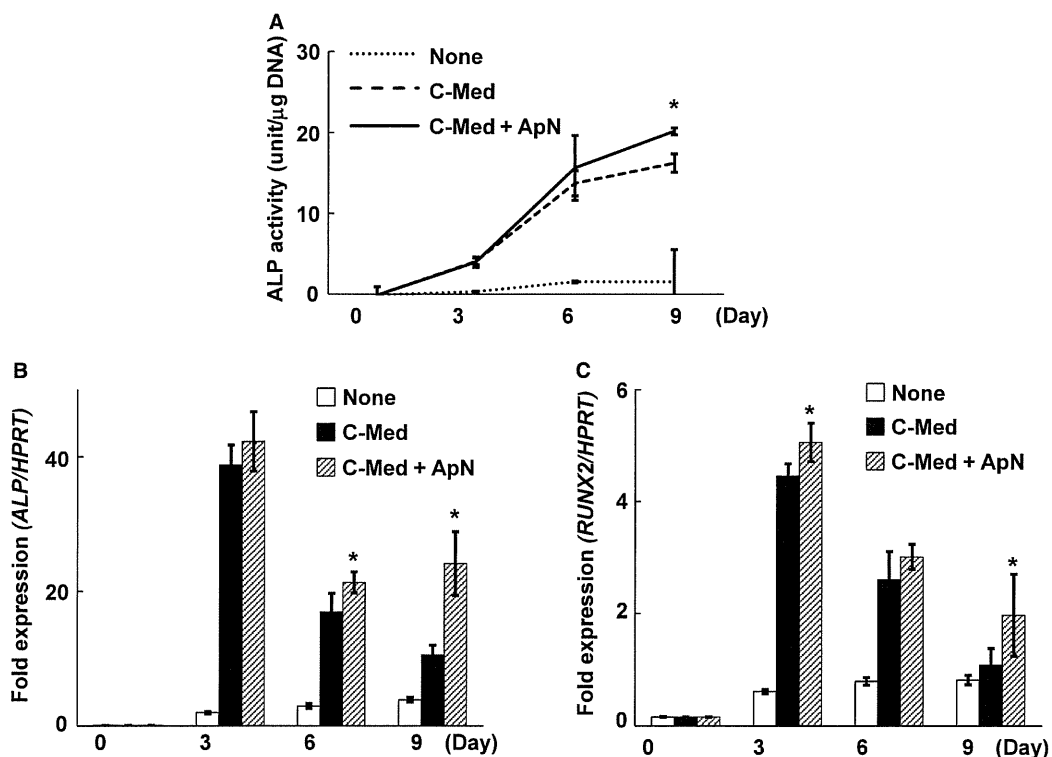

Fig. 6. Adiponectin promoted the differentiation of human periodontal ligament (HPDL) cells. (A) HPDL cells were cultured in calcification-induced medium (C-Med) in the presence or absence of adiponectin (ApN; 10 μg/mL) for the indicated periods of time, then alkaline phosphatase (ALP) activity during the cytodifferentiation of HPDL cells was measured. Data are the mean ± standard deviation of triplicate determinations. *p < 0.05 compared with HPDL cells cultured in C-Med in the absence of ApN. (B and C) Real-time PCR was performed to determine the expression of cytodifferentiation- and mineralization-related genes, such as *ALP* (B) and runt-related transcription factor 2 (*RUNX2*) (C). HPDL cells were cultured in C-Med in the presence or absence of adiponectin (ApN; 10 μg/mL) for the indicated periods of time. Data are the mean ± standard deviation of triplicate determinations. *p < 0.05 compared with HPDL cells cultured in C-Med in the absence of adiponectin. HPRT, hypoxanthine phosphoribosyltransferase.
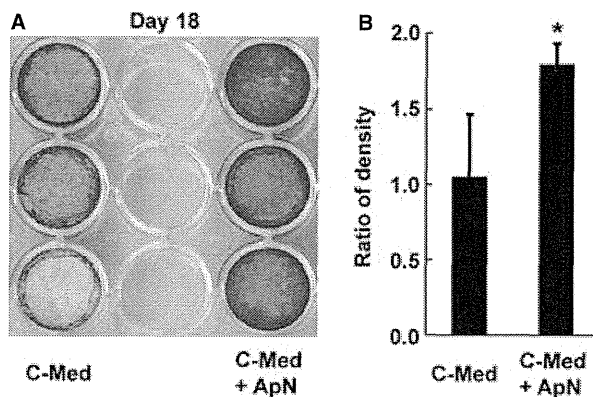
Fig. 7. Adiponectin promoted the mineralization of human periodontal ligament (HPDL) cells. (A) Mineralized nodule formation in HPDLs was detected by staining the cells with Alizarin Red after 18 d of culture in calcification-induced medium (C-Med) in the presence or absence of adiponectin (ApN; 10 μg/mL). (B) The relative expression value of Alizarin Red staining is shown in (A) and was quantified and normalized to Alizarin Red staining without C-Med. The data represent one of three independent experiments. $*p < 0.05$ compared with C-Med only.

stimulated via AdipoR1 and induces the production of bone morphogenetic protein-2, stimulating cells to differentiate into calcified (26,30). Further studies are necessary to clarify the involvement of the SIRT1 and AMPK signaling pathways in the action of adiponectin on both gingival fibroblasts and HPDL cells.

In summary, the results of the present study suggest that adiponectin may have a therapeutically beneficial effect on the control of anti-inflammatory responses and treatment of periodontal diseases. Topical application of recombinant adiponectin during periodontal surgery may improve wound healing and regeneration at the periodontal disease site. Further studies are still required to demonstrate this therapeutic effect.

Acknowledgements

References

1. Garcia RI, Henshaw MM, Krall EA. Relationship between periodontal disease and systemic health. *Periodontol 2000* 2001;**25**:21–36.

2. Saito T, Shimazaki Y, Sakamoto M. Obesity and periodontitis. *N Engl J Med* 1998;**339**:482–483.

3. Chaffee BW, Weston SJ. Association between chronic periodontal disease and obesity: a systematic review and meta-analysis. *J Periodontol* 2010;**81**:1708–1724.

4. Kopelman PG. Obesity as a medical problem. *Nature* 2000;**404**:635–643.

5. Funahashi T, Nakamura T, Shimomura I et al. Role of adipocytokines on the pathogenesis of atherosclerosis in visceral obesity. *Intern Med* 1999;**38**:202–206.

6. Scherer PE, Williams S, Fogliano M, Baldini G, Lodish HF. A novel serum protein similar to C1q, produced exclusively in adipocytes. *J Biol Chem* 1995;**270**:26746–26749.

7. Yamauchi T, Kamon J, Ito Y et al. Cloning of adiponectin receptors that mediate antidiabetic metabolic effects. *Nature* 2003;**423**:762–769.

8. Ouchi N, Kihara S, Arita Y et al. Novel modulator for endothelial adhesion molecules: adipocyte-derived plasma protein adiponecti. *Circulation* 1999;**100**:2473–2476.

9. Yu JG, Javorschi S, Hevener AL et al. The effect of thiazolidinediones on plasma adiponectin levels in normal, obese, and type 2 diabetic subjects. *Diabetes* 2002;**51**:2968–2974.

10. Ouchi N, Parker JL, Lugus JJ, Walsh K. Adipokines in inflammation and metabolic disease. *Nat Rev Immunol* 2011;**11**: 85–97.

11. Saito T, Yamaguchi N, Shimazaki Y et al. Serum levels of resistin and adiponectin in women with periodontitis: the Hisayama study. *J Dent Res* 2008;**87**:319–322.

12. Furugen R, Hayashida H, Yamaguchi N et al. The relationship between periodontal condition and serum levels of resistin and adiponectin in elderly Japanese. *J Periodontal Res* 2008;**43**:556–562.

13. Kardeşler L, Buduneli N, Cetinkalp S, Kinane DF. Adipokines and inflammatory mediators after initial periodontal treatment in patients with type 2 diabetes and chronic periodontitis. *J Periodontol* 2010;**81**:24–33.

14. Yamaguchi N, Hamachi T, Kamio N et al. Expression levels of adiponectin receptors and periodontitis. *J Periodontal Res* 2010;**45**:296–300.

15. Berner HS, Lyngstadaas SP, Spahr A et al. Adiponectin and its receptors are expressed in bone-forming cells. *Bone* 2004;**35**:842–849.

16. Oshima K, Nampei A, Matsuda M et al. Adiponectin increases bone mass by suppressing osteoclast and activating osteoblast. *Biochem Biophys Res Commun* 2005;**331**:520–526.

17. Seo BM, Miura M, Gronthos S et al. Investigation of multipotent postnatal stem cells from human periodontal ligament. *Lancet* 2004;**364**:149–155.

18. Murakami S, Hashikawa T, Saho T et al. Adenosine regulates the IL-1 beta-induced cellular functions of human gingival fibroblasts. *Int Immunol* 2001;**13**:1533–1540.

19. Somerman MJ, Archer SY, Imm GR, Foster RA. A comparative study of human periodontal ligament cells and gingival fibroblasts in vitro. *J Dent Res* 1988;**67**:66–70.

20. Fujihara C, Yamada S, Ozaki N et al. Role of mechanical stress-induced glutamate signaling-associated molecules in cytodifferentiation of periodontal ligament cells. *J Biol Chem* 2010;**285**:28286–28297.

21. Bessey OA, Lowly OH, Brock MJ. A method for the rapid determination of alkaline phosphates with five cubic millimeters of serum. *J Biol Chem* 1946; **164**:321–329.

22. Dahl LK. A simple and sensitive histochemical method for calcium. *Proc Soc Exp Biol Med* 1952;**80**:474–479.

23. Yang S, Wei D, Wang D, Phimphilai M, Krebsbach PH, Franceschi RT. In vitro and in vivo synergistic interactions between the Runx2/Cbfa1 transcription factor and bone morphogenetic protein-2 in stimulating osteoblast differentiation. *J Bone Miner Res* 2003;**18**:705–715.

24. Arita Y, Kihara S, Ouchi N et al. Paradoxical decrease of an adipose-specific protein, adiponectin, in obesity. *Biochem Biophys Res Commun* 1999;**257**:79–83.

25. Lee SW, Kim JH, Park MC, Park YB, Lee SK. Adiponectin mitigates the severity of arthritis in mice with collagen-induced

arthritis. *Scand J Rheumatol* 2008;**37**:260–268.

26. Kanazawa I, Yamaguchi T, Yano S, Yamauchi M, Yamamoto M, Sugimoto T. Adiponectin and AMP kinase activator stimulate proliferation, differentiation, and mineralization of osteoblastic MC3T3-E1 cells. *BMC Cell Biol* 2007;**8**:51.

27. Majeska RJ, Wuthier RE. Studies on matrix vesicles isolated from chick epiphyseal cartilage. Association of pyrophosphatase and ATPase activities with alkaline phosphatase. *Biochim Biophys Acta* 1975;**391**:51–60.

28. Yang SR, Wright J, Bauter M, Seweryniak K, Kode A, Rahman I. Sirtuin regulates cigarette smoke-induced proinflammatory mediator release via RelA/p65 NF-kappaB in macrophages in vitro and in rat lungs in vivo: implications for chronic inflammation and aging. *Am J Physiol Lung Cell Mol Physiol* 2007;**292**:L567–L576.

29. Shen Z, Ajmo JM, Rogers CQ *et al.* Role of SIRT1 in regulation of LPS- or two ethanol metabolites-induced TNF-alpha production in cultured macrophage cell lines. *Am J Physiol Gastrointest Liver Physiol* 2009;**296**:G1047–G1053.

30. Huang CY, Lee CY, Chen MY, Tsai HC, Hsu HC, Tang CH. Adiponectin increases BMP-2 expression in osteoblasts via AdipoR receptor signaling pathway. *J Cell Physiol* 2010;**224**:475–483.

CD73-Generated Adenosine Promotes Osteoblast Differentiation

MASAHIDE TAKEDACHI,[1,2] HIROYUKI OOHARA,[1] BRENDA J. SMITH,[3] MITSUYOSHI IYAMA,[1] MARIKO KOBASHI,[1] KENICHIRO MAEDA,[1] COURTNEY L. LONG,[4] MARY B. HUMPHREY,[5] BARBARA J. STOECKER,[3] SATORU TOYOSAWA,[2] LINDA F. THOMPSON,[6] AND SHINYA MURAKAMI[1]*

[1] Department of Periodontology, Osaka University Graduate School of Dentistry, Osaka, Japan

[2] Department of Oral Pathology, Osaka University Graduate School of Dentistry, Osaka, Japan

[3] Department of Nutritional Sciences, Oklahoma State University, Stillwater, Oklahoma

[4] Department of Microbiology and Immunology, University of Oklahoma Health Sciences Center, Oklahoma City, Oklahoma

[5] Department of Medicine, University of Oklahoma Health Sciences Center, Oklahoma City, Oklahoma

[6] Department of Immunobiology and Cancer Program, Oklahoma Medical Research Foundation, Oklahoma City, Oklahoma

CD73I is a GPI-anchored cell surface protein with ecto-5′-nucleotidase enzyme activity that plays a crucial role in adenosine production. While the roles of adenosine receptors (AR) on osteoblasts and osteoclasts have been unveiled to some extent, the roles of CD73 and CD73-generated adenosine in bone tissue are largely unknown. To address this issue, we first analyzed the bone phenotype of CD73-deficient ($cd73^{-/-}$) mice. The mutant male mice showed osteopenia, with significant decreases of osteoblastic markers. Levels of osteoclastic markers were, however, comparable to those of wild-type mice. A series of in vitro studies revealed that CD73 deficiency resulted in impairment in osteoblast differentiation but not in the number of osteoblast progenitors. In addition, over expression of CD73 on MC3T3-E1 cells resulted in enhanced osteoblastic differentiation. Moreover, MC3T3-E1 cells expressed adenosine A_{2A} receptors ($A_{2A}AR$) and A_{2B} receptors ($A_{2B}AR$) and expression of these receptors increased with osteoblastic differentiation. Enhanced expression of osteocalcin (OC) and bone sialoprotein (BSP) observed in MC3T3-E1 cells over expressing CD73 were suppressed by treatment with an $A_{2B}AR$ antagonist but not with an $A_{2A}AR$ antagonist. Collectively, our results indicate that CD73 generated adenosine positively regulates osteoblast differentiation via $A_{2B}AR$ signaling.
J. Cell. Physiol. 227: 2622–2631, 2012. © 2011 Wiley Periodicals, Inc.

A balanced relationship between bone resorption by osteoclasts and bone formation by osteoblasts is essential for bone remodeling which maintains bone integrity. The extracellular nucleotide ATP can be one of the key mediators in bone metabolism, not only as a phosphate source, but also as a signaling molecule via P2 receptors. In fact, osteoblasts have been reported to release ATP into the extracellular environment constitutively followed by engagement of P2 receptors (Buckley et al., 2003). The release of ATP by osteoblasts could be facilitated by mechanical stress (Romanello et al., 2001) and released ATP serves as an autocrine or paracrine regulator of both osteoblast and osteoclast function (Grol et al., 2009; Orriss et al., 2010). Meanwhile, it has been reported that P2 receptor signal transduction is rapidly inactivated by the extracellular breakdown of ATP to adenosine by the sequential actions of enzymes including members of the ecto-nucleoside triphosphate diphosphohydrolase and ecto-nucleotide pyrophosphatase/phosphodiesterase families, ecto-5′-nucleotidase (CD73) and alkaline phosphatases (ALPase; Yegutkin, 2008). Although the role of ATP in bone metabolism has been revealed to some extent, functions of its metabolite adenosine are not fully elucidated.

The biological actions of adenosine are mediated via A_1, A_{2A}, A_{2B}, and A_3 adenosine receptors (AR) that are ubiquitously expressed seven transmembrane spanning G-protein-coupled receptors. A_1AR and A_3AR mediate an inhibitory effect on adenylyl cyclase via Gi/Go, resulting in decreasing cAMP levels, whereas, A_{2A} receptors ($A_{2A}AR$)

and A_{2B} receptors ($A_{2B}AR$) stimulate adenylyl cyclase via activation of Gs with a consequent increase of cAMP (Ralevic and Burnstock, 1998). Recent reports suggested that adenosine supports osteoclast formation and bone resorption. It was shown that A_1AR signaling was required for osteoclastogenesis in vitro (Kara et al., 2010b) and lack of A_1AR resulted in increased bone mass in mice (Kara et al., 2010a). In addition, Evans et al. (2006) demonstrated that AR activation inhibited osteoprotegerin expression but did not affect receptor activator of NF-κB ligand expression in human osteoblasts. On the other hand, several in vitro studies demonstrated the role of

adenosine in osteoblasts. Engagement of AR on murine osteoblasts induced mitogenesis (Shimegi, 1998; Fatokun et al., 2006) and protected them from cell death (Fatokun et al., 2006). In addition, selective agonists specific for each AR subtype modulated proliferation and osteogenic differentiation of human bone marrow stromal cells (Costa et al., 2010, 2011). Although these reports strongly suggest that AR signaling may play a critical role in osteoblasts, no report provides in vivo evidence.

AR activation is believed to be regulated by the extracellular adenosine level which is controlled by the coordinated action of an equilibrative nucleoside transporter and ecto-nucleotidases. CD73 is a major enzyme involved in the generation of extracellular adenosine by the dephosphorylation of adenosine 5′-monophosphate (Thomson et al., 1990). Although cytoplasmic nucleotidases also make a contribution to adenosine production, recent studies utilizing $cd73^{-/-}$ mice clearly demonstrated that CD73 plays a major role in the generation of extracellular adenosine in vivo in a number of physiologically relevant experimental models (Thompson et al., 2004; Volmer et al., 2006; Eckle et al., 2007; Takedachi et al., 2008). Interestingly, CD73 expression is regulated by Wnt-β-catenin signaling (Spychala and Kitajewski, 2004), a known critical pathway in bone metabolism (Baron et al., 2006; Piters et al., 2008; Williams and Insogna, 2009). It is also noteworthy that hypoxia inducible factor-1α (HIF-1α), a transcription factor reported to be important for bone regeneration and skeletal development (Wang et al., 2007; Wan et al., 2008), also regulates CD73 expression (Synnestvedt et al., 2002). Therefore, we hypothesized that CD73 may be involved in regulating osteoblast function through modulating nucleotide metabolism and generating extracellular adenosine that can activate AR.

To address this hypothesis, we asked whether CD73 functionally regulates bone metabolism in vivo by characterizing the bone phenotype of $cd73^{-/-}$ mice. In addition, we investigated the involvement of CD73 and AR signaling in osteoblast differentiation in vitro.

Materials and Methods
Mice

$cd73^{-/-}$ mice were developed as described (Thompson et al., 2004) and backcrossed onto the C57BL/6J background for 14 generations. Genotyping was performed by polymerase chain reaction (PCR) using DNA extracted from toes and primers that differentiate between the wild-type $cd73$ allele and the mutated $cd73$ allele containing a neomycin resistance cassette (Thompson et al., 2004). All mice were bred and maintained in our animal facilities under specific pathogen-free (SPF) conditions. All protocols were approved by the Institutional Animal Care and Use Committees of the Oklahoma Medical Research Foundation and Osaka University Graduate School of Dentistry.

Peripheral quantitative computed tomography (pQCT) and micro-computed tomography (μCT)

In pQCT analyses, femurs were harvested from $cd73^{+/+}$ and $cd73^{-/-}$ male and female mice at 13 weeks of age and were fixed with 10% buffered formalin for 24 h and analyzed using an XCT Research SA+ instrument (Stratec Medizintechnik GmbH, Pforzheim, Germany). Voxel size was 0.08 mm × 0.08 mm × 0.46 mm. The contour of the total bone was determined automatically by the pQCT software algorithm. The parameters were obtained at 1.2 mm from the distal growth plate using threshold values of 690 mg/cm³ for the cortical region and 395 mg/cm³ for the trabecular region.

In μCT analyses, tibias from 13-week-old $cd73^{+/+}$ and $cd73^{-/-}$ male mice were scanned using μCT (μCT40, SCANCO Medical, Bruttisellen, Switzerland) to assess trabecular bone

microarchitecture at the proximal tibia metaphysis. Scans of the proximal tibia metaphysis were performed at a resolution of 2,048 pixels × 2,048 pixels. Analyses of the proximal tibia were accomplished by placing semiautomated contours beginning 0.03 mm distal to the growth plate and including a 0.6 mm volume of interest (VOI) of only secondary spongiosa for trabecular analyses. All samples were evaluated at a global threshold of 300 in the per mille unit to segment mineralized from soft tissue. Trabecular parameters evaluated included bone volume expressed per unit of total volume (BV/TV; %), trabecular number (TbN; 1/mm), trabecular thickness (TbTh; μm), and trabecular separation (TbSp; μm).

Histology and immunohistochemistry

For histological analysis, tibias were dissected from 13-week-old $cd73^{+/+}$ and $cd73^{-/-}$ male mice and fixed overnight at 4°C in 10% formalin in PBS, decalcified in 10% EDTA at 4°C for 10 days, and embedded in paraffin. Sections (4 μm) were prepared and stained with hematoxylin and eosin (H&E). For immunohistochemistry, calvaria were collected from 3-day-old $cd73^{+/+}$ and $cd73^{-/-}$ male mice and fixed overnight at 4°C in 4% paraformaldehyde in PBS, decalcified in 7.5% EDTA at 4°C for 14 days, and embedded in OCT compound (Sakura Finetek Co., Ltd., Tokyo, Japan). Then 7 μm frozen sections were prepared and treated with 2.5% hyaluronidase (Sigma–Aldrich, St. Louis, MO) in PBS at 37°C for 1 h, followed by inactivation of endogenous peroxidase with 0.3% H_2O_2 in PBS containing 0.3% FBS (Nichirei Biosciences, Tokyo, Japan). After blocking with 3% BSA in PBS overnight at 4°C, sections were reacted with 5 μg/ml rat anti-mouse CD73 antibody (TY/23; Yamashita et al., 1998; BD Pharmingen, Franklin Lakes, NJ). After washing, they were then incubated with biotin-conjugated anti-rat IgG, treated with the ABC reagents (Vector Laboratories, Inc., Burlingame, CA), developed with DAB (Dojindo, Kumamoto, Japan) and counterstained with hematoxylin.

Serum measurements

OC, tartrate-resistant acid phosphatase isoform 5b (TRAP5b), C-teminal telopeptide of type I collagen, and phosphate were measured in mouse sera collected from 13-week-old $cd73^{+/+}$ and $cd73^{-/-}$ male mice after an overnight fast. OC was determined by sandwich ELISA using the mouse osteocalcin (OC) EIA kit (Biomedical Technologies Inc., Stoughton, MA). TRAP5b level was determined by a solid phase immunofixed enzyme activity assay using the MouseTRAP Assay kit (IDS Ltd., Boldon, UK). C-teminal telopeptide of type I collagen was measured by RatLaps ELISA kit (Nordic Bioscience Diagnostics, Herlev, Denmark) using a rabbit polyclonal antibody raised against a synthetic peptide having a sequence specific for a part of the C-terminal telopeptide α1 chain of rat type I collagen. Serum inorganic phosphate was determined by the improved Malachite Green method utilizing the malachite green dye and molybdate provided by the Phosphate assay kit (BioChain, Hayward, CA).

Reverse transcription (RT)-PCR

Total RNA was extracted from calvarial or femoral bones of 13-week-old $cd73^{-/-}$ male mice and wild-type control mice by TissueLyser II (Retch, Haan D, Germany) or from in vitro cultured cells using RNA-Bee (TEL-TEST, Inc., Friendwood, TX) in accordance with the manufacturer's instructions. Purified total RNA was reverse-transcribed using M-MLV (Invitrogen, Carlsbad, CA) reverse transcriptase with random hexamers. For semiquantitative analysis, PCR was carried out using AmpliTaq Gold DNA polymerase (Roche Applied Science, Indianapolis, IN). The primer sequences used for semiquantitative PCR are previously described (Van De Wiele et al., 2002). Real-time PCR analysis was performed using Power SYBR Green PCR Master Mix and a 7300 Fast Real-Time PCR system (Applied Biosystems, Foster

City, CA). The primer sequences used for Real-Time PCR are listed in Table 1.

Cell culture and transfection

Primary osteoblasts were isolated from 3-day-old pups by digesting calvarial bones in PBS containing 0.1% collagenase (Wako Pure Chemical Industries, Osaka, Japan) and 0.2% dispase (Roche Applied Science) for 20 min at 37°C. The digestion was sequentially performed three times and cells isolated from last two digestion were cultured in α-MEM supplemented with 10% FBS as primary osteoblasts. MC3T3-E1 cells were obtained from the Riken Cell Bank (Tsukuba, Japan). Cells were maintained in α-MEM (Nikken Biomedical Laboratory, Kyoto, Japan) supplemented with 10% FBS and 60 μg/ml kanamycin. To induce differentiation, cells were cultured in a 24-well plates until they reached confluence and then switched to mineralization medium (α-MEM supplemented with 10% FBS, 10 mM β-glycerophosphate, and 50 μg/ml ascorbic acid) which was replaced every 3 days.

To produce stable transfectants, 2×10^4 MC3T3-E1 cells/well were plated in a 24-well plates and after 24 h, were transfected with the pHβ Apr-1-neo-cd73 expression vector (Resta et al., 1994) using Lipofectamine 2000 (Invitrogen) in accordance with the manufacturer's protocol. After 24 h, the culture medium was supplemented with 600 μg/ml geneticin (Invitrogen) to initiate drug selection. After selection, we then established the stable transfectant over expressing CD73 (MC/CD73). Cells used in this study had been passaged 3–5 times.

Colony forming assay

Bone marrow cells were flushed with PBS from femurs and tibias of 13-week-old $cd73^{+/+}$ and $cd73^{-/-}$ mice. One million bone marrow cells/well were plated in a 6-well plates and cultured in α-MEM supplemented with 10% FBS for 14 days. The cells were fixed with methanol and stained with Giemsa (Wako Pure Chemical Industries). Colonies with >20 cells were counted as fibroblast colony forming units (CFU-F). To enumerate osteoblast colony forming units (CFU-OB), bone marrow cells were cultured in mineralization media for 10 days and fixed with ethanol. Formation of osteoblast progenitors were detected using an ALPase staining kit (Sigma–Aldrich) and ALPase positive colonies with >20 cells were counted. Then Giemsa staining was performed and total colonies were counted. CFU-OB was calculated as a ratio of ALPase positive colonies/total colonies.

Flow cytometry analysis

Single cell suspensions of MC/CD73 or control transfectants were prepared by trypsinization and reacted with 10 μg/ml PE-conjugated rat anti-CD73 antibody TY/23 (BD Pharmingen) or an isotype-matched control antibody. Data were collected with a

FACSCalibur (BD Biosciences, San Jose, CA) and analyzed with CellQuest software.

Proliferation assay

Proliferation of MC/CD73 and control transfectants was measured using the nonradioactive colorimetric WST-1 Cell Proliferation Assay (Roche Applied Science) according to the manufacturer's instructions. This assay is based on the cleavage of a tetrazolium salt by mitochondrial dehydrogenases to form formazan in viable cells. Briefly, 1×10^4 cells were plated in 24-well plates and cultured in α-MEM supplemented with 10% FBS. The number of viable cells was determined by adding WST-1 reagent and colorimetric evaluation of OD450/630 by a microplate reader (Bio-Rad, Hercules, CA) after 30 min incubation.

ALPase activity

After washing twice with PBS, the cells were sonicated in 0.01 M Tris/HCl (pH 7.4) and then centrifuged for 5 min at $12,000 \times g$. Subsequently the supernatant was mixed with 0.5 M Tris–HCl buffer (pH 9.0) containing 0.5 mM p-nitrophenyl phosphate as substrate, 0.5 mM $MgCl_2$, and 0.006% Triton X-100. Then the samples were incubated at room temperature for 60 min, and the reaction was stopped by addition of 0.2 M NaOH. The hydrolysis of p-nitrophenyl phosphate was monitored as a change in OD410. ALPase from bovine intestinal mucosa was used as a standard and one unit of activity was defined as the enzyme activity hydrolyzing 1 μmol of p-nitrophenyl phosphate per min at pH 9.8 at 37°C. Protein concentration was determined by Lowry method and the results were expressed as mU/μg protein.

Mineralization assay

Histochemical staining of calcified nodules was performed with alizarin red S. Cell monolayers were washed twice with PBS, and then fixed with dehydrated ethanol. After fixation, the cell layers were stained with 1% alizarin red S in 0.1% NH_4OH (pH 6.5) for 5 min, then washed with H_2O.

cAMP measurement

Cells were washed with serum-free α-MEM and treated with 0.1% DMSO (as carrier) or 10 nM to 1 μM of the $A_{2A}AR$ antagonist ZM241385 (Tocris Bioscience, Ellisville, MO) or 10 nM to 1 μM of the $A_{2B}AR$ antagonist MRS1754 (Sigma–Aldrich). After 10 min incubation, cells were stimulated with 100 μM adenosine (Sigma–Aldrich) for 5 min. Intracellular cAMP was determined by competition between cAMP of cells and cAMP conjugated to ALPase detected by rabbit polyclonal antibody to cAMP using a cyclic AMP complete EIA kit (Assay Designs, Ann Arbor, MI). Protein concentration was determined by the Lowry method and the cAMP results were expressed in pmol/mg protein.

TABLE 1. Nucleotide sequences of primers used for PCR

Gene	Product size (bp)		Primer sequence
Beta actin	171	F	5'-CATCCGTAAAGACCTCTATGCCAAC-3'
		R	5'-ATGGAGCCACCGATCCACA-3'
Runt related transcription factor 2	144	F	5'-CACTGGCGGTGCAACAAGA-3'
		R	5'-TTTCATAACAGCGGAGGCATTTC-3'
Bone sialoprotein	153	F	5'-ATGGAGACTGCGATAGTTCCGAAG-3'
		R	5'-CGTAGCTAGCTGTTACACCCGAGAG-3'
Osteocalcin	178	F	5'-AGCAGCTTGGCCCAGACCTA-3'
		R	5'-TAGCGCCGGAGTCTGTTCACTAC-3'
Alkaline phosphatase	159	F	5'-ACACCTTGACTGTGGTTACTGCTGA-3'
		R	5'-CCTTGTAGCCAGGCCCGTTA-3'
CD73 (5'-nucleotidase, ecto)	118	F	5'-AGTTCGAGGTGTGGACATCGTG-3'
		R	5'-ATCATCTGCGGTGACTATGAATGG-3'
Adenosine A2a receptor	172	F	5'-ATTCGCCATCACCATCAGCA-3'
		R	5'-ACCCGTCACCAAGCCATTGTA-3'
Adenosine A2b receptor	157	F	5'-GTCGACCGATATCTGGCCATTC-3'
		R	5'-TGCTGGTGGCACTGTCTTTACTG-3'

Statistical analysis

Data were expressed as the mean ± SE. Statistical analyses were performed by Student's t-test. In some experiments, statistical analyses were performed by one-way ANOVA and specific differences were identified by the Bonferroni test: $P < 0.05$ was considered statistically significant.

Results

CD73 is expressed in periosteal osteoblasts

To determine where CD73 is expressed in bone tissue, frozen sections of calvaria specimens from 3-day-old $cd73^{+/+}$ mice were examined. Incubation with anti-CD73 antibody (TY/23) demonstrated that periosteum containing osteoblast and osteoblast precursors expressed CD73 (Fig. 1A). In contrast, no CD73 expression was observed in the periosteum of $cd73^{-/-}$ mice.

$cd73^{-/-}$ mice exhibit osteopenia

To examine the skeletal phenotype of 13-week-old $cd73^{-/-}$ mice, we first evaluated the bone mineral density by pQCT. Compared to control littermates, male $cd73^{-/-}$ mice had significantly lower bone mineral content in the trabecular bone of the femur metaphysis (Table 2). No differences were observed in the trabecular bone of female $cd73^{-/-}$ or cortical bone of either male or female mice at the femur diaphysis. Histological evaluation of the proximal tibias showed that $cd73^{-/-}$ male mice exhibited small and scattered bone spicules in the proximal metaphysis area compared with sex-matched wild-type mice (Fig. 1B).

Quantitative analyses of trabecular bone were accomplished using μCT. Representative three-dimensional images reconstructed from μCT scans of trabecular bone at the proximal tibia metaphysis further demonstrated osteopenia in male $cd73^{-/-}$ mice (Fig. 1C). These changes were characterized by reduced trabecular bone volume, decreased trabecular number and thickness (Fig. 1D), and increased trabecular separation (data not shown) in $cd73^{-/-}$ mice.

$cd73^{-/-}$ mice exhibit decreased bone formation and osteoblast differentiation in vivo

We then investigated whether osteopenia in male $cd73^{-/-}$ mice was the result of impaired bone formation or activated bone resorption. To address this question, we measured biochemical markers of in vivo bone turnover. As shown in Figure 2A, a significant decrease in serum OC, a metabolic marker of in vivo bone formation (Hauschka et al., 1989), was observed in $cd73^{-/-}$ mice. In contrast, levels of the osteoclast marker TRAP5b (Alatalo et al., 2003) and fragments of type I collagen (C-terminal telopeptide), the products of bone resorption (Garnero et al., 2003), were comparable in the two strains of mice.

To further substantiate the involvement of impaired osteoblasts in the phenotype of $cd73^{-/-}$ mice, we investigated the gene expression of osteoblast markers in calvarial and femoral bones. Real-time PCR analysis demonstrated significantly decreased expression of Runx2, ALPase, OC, and bone sialoprotein (BSP) in calvarial and femoral bones of $cd73^{-/-}$ mice (Fig. 2B,C). These results suggested that the involvement of CD73 in bone homeostasis was directed to the osteoblast.

Inorganic phosphate required for osteoblast differentiation and mineralization (Beck, 2003) is produced when CD73 catalyzes the conversion of adenosine monophosphate to adenosine. To examine if decreased inorganic phosphate contributed to the reduction in trabecular bone volume in $cd73^{-/-}$ mice, serum phosphate was determined. As shown in Figure 2A, serum phosphate in $cd73^{-/-}$ mice was similar to that
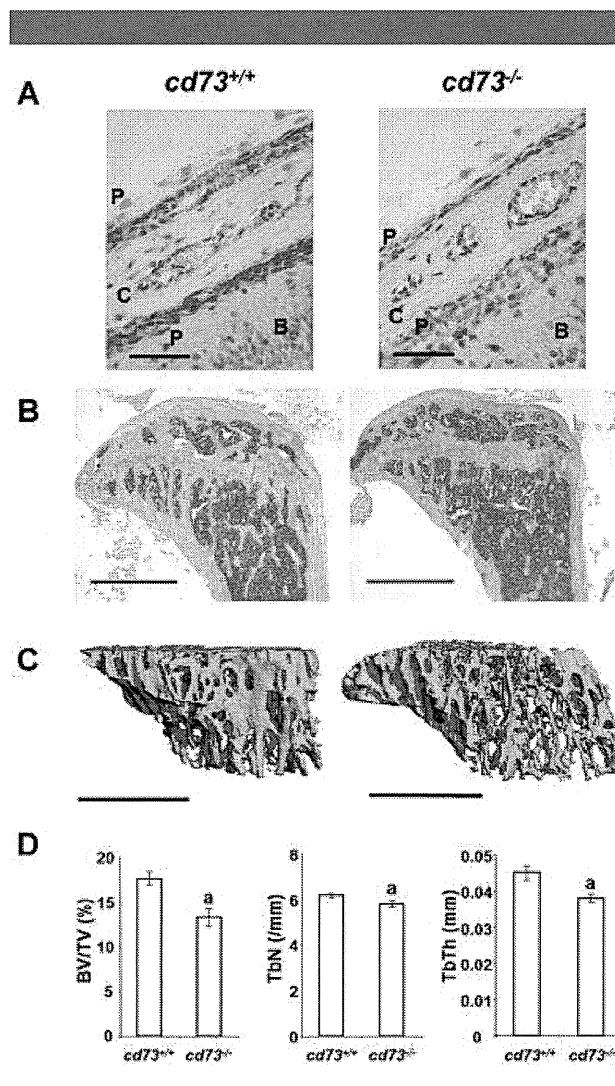

Fig. 1. Bone phenotype of $cd73^{-/-}$ mice. A: CD73 expression on periosteum. Frozen sections of calvarial bones from $cd73^{+/+}$ and $cd73^{-/-}$ mice at 3 days of age were incubated with anti-CD73 monoclonal antibody (TY/23) and developed with DAB, as described in the Materials and Methods Section. P, periosteum; C, calvarial bone; B, brain. Scale bar, 50 μm. Representative images of (B) H&E-stained medial, longitudinal sections of proximal tibias and (C) μCT reconstruction of the proximal tibial metaphysis of $cd73^{+/+}$ and $cd73^{-/-}$ mice at 13 weeks of age. Scale bar (B) and (C), 1 mm. D: Histomorphometric analysis of trabecular bone volume per tissue volume (BV/TV), trabecular number (TbN), and trabecular thickness (TbTh) of secondary spongiosa in $cd73^{+/+}$ and $cd73^{-/-}$ mice (n = 7–8/ each group). Data are expressed as mean ± SE. $^{a}P < 0.05$ compared with $cd73^{+/+}$ mice.

TABLE 2. Cortical and trabecular bone mineral density at the distal femur metaphysis and body weights of $cd73^{-/-}$ and $cd73^{+/+}$ male and female mice

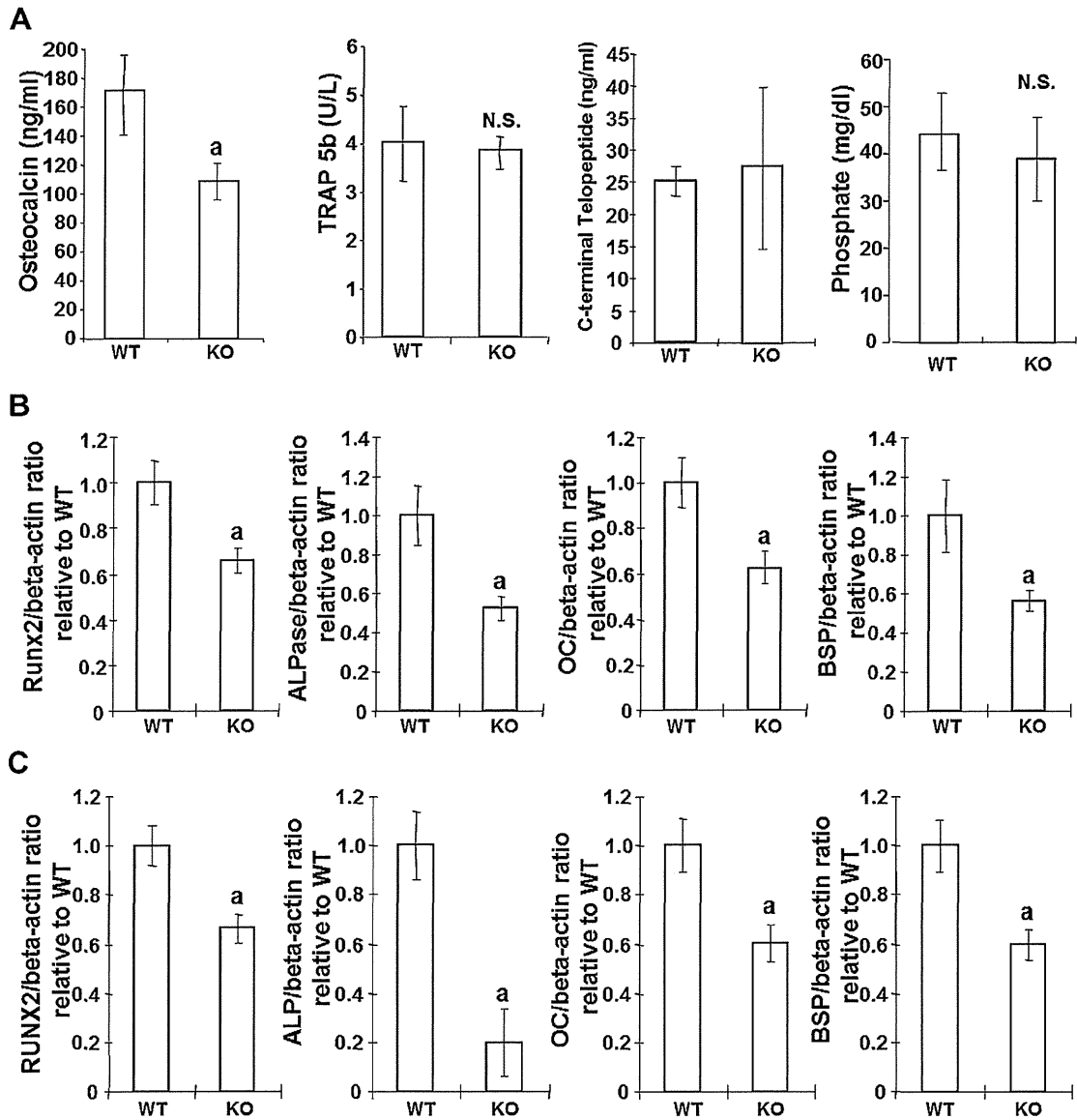|	Genotype	Bone mineral density (mg/cm³)		Body weight (g)
		Trabecular bone	Cortical bone	
Male	CD73$^{+/+}$	271.15 ± 23.09	1081.48 ± 18.77	27.32 ± 1.57
	CD73$^{-/-}$	246.13 ± 13.78[a]	1070.55 ± 25.78	27.52 ± 1.48
Female	CD73$^{+/+}$	206.23 ± 23.03	1051.62 ± 18.13	19.23 ± 2.14
	CD73$^{-/-}$	207.39 ± 21.65	1055.03 ± 20.64	19.43 ± 0.64

[a]$P < 0.05$ compared with $cd73^{+/+}$ mice.

114

Fig. 2. Decreased osteoblast markers in cd73^{−/−} mice. A: Serum OC, TRAP5b, C-terminal telopeptides, and inorganic phosphate in cd73^{+/+} and cd73^{−/−} mice at 13 weeks of age. Gene expression of Runx2, ALPase, OC, and BSP mRNA in femoral (B) and calvarial (C) bone samples from cd73^{+/+} and cd73^{−/−} mice as determined by real-time PCR (n = 6–13 in each group). Results were normalized to β-actin mRNA levels in the same samples. Data are expressed as mean ± SE. [a]$P < 0.05$ compared with cd73^{+/+} mice.

in cd73^{+/+} mice, suggesting that CD73 has a minor role in production of phosphates.

CD73 deficiency impairs osteoblast differentiation in vitro

Ex vivo studies were performed to identify the role of CD73 in osteoblasts differentiation and mineralization. Primary osteoblasts were isolated from calvarial bones of cd73^{+/+} mice and cd73^{−/−} mice and cultured in mineralization medium to examine the role of CD73 in osteoblast differentiation. As shown in Figure 3A, ALPase mRNA expression and activity were significantly decreased in CD73-deficient osteoblasts

compared to wild-type osteoblasts at 6 days of culture. Moreover, calcified nodule formation was delayed in cultures from cd73^{−/−} mice, suggestive of reduced mineralization (Fig. 3B).

Because $A_{2A}AR$ is reported to play a role in bone marrow-derived mesenchymal stem cell development (Katebi et al., 2009), we assessed the number of bone marrow stem cells and osteoblast progenitors in bone marrow of cd73^{−/−} mice. Colony forming assays revealed that bone marrow cells cultured from cd73^{−/−} mice formed similar numbers of fibroblast colonies and ALPase positive osteoblast colonies compared to cultures from cd73^{+/+} mice (Fig. 3C). Taken together, our results suggested that CD73 plays a role in
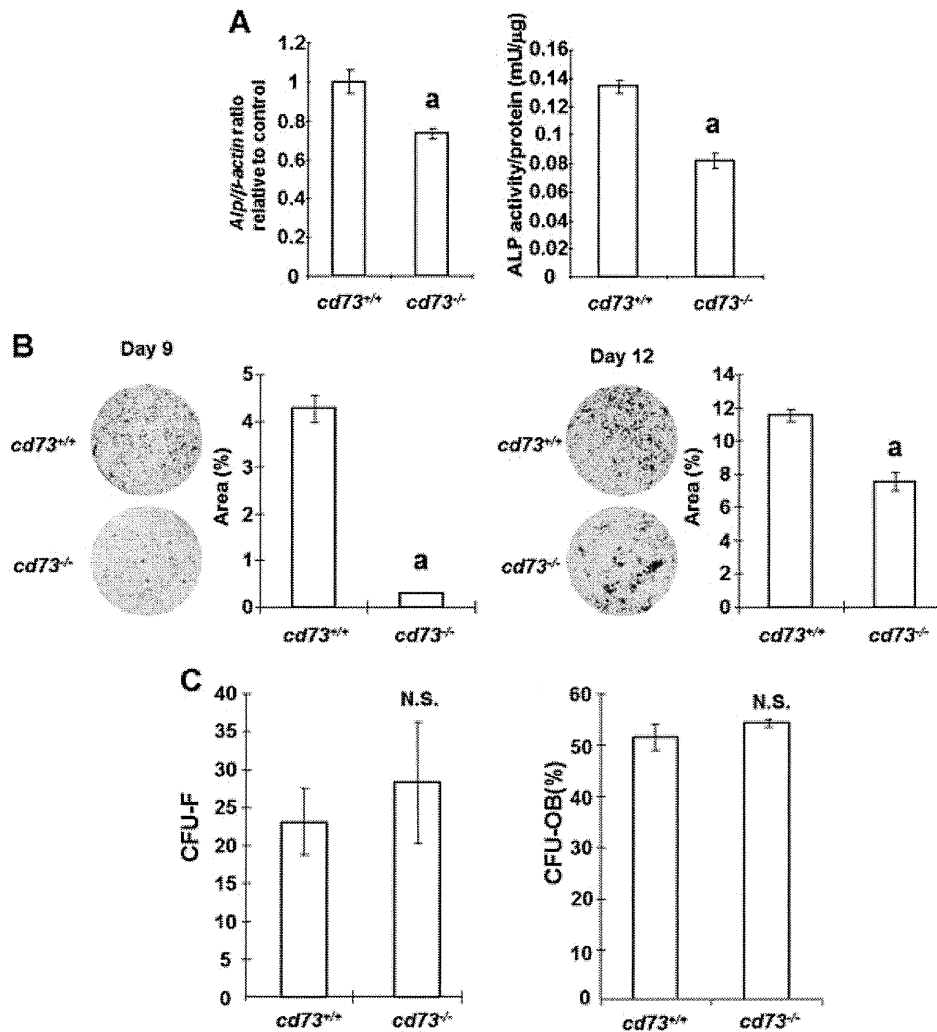
Fig. 3. Impaired differentiation in CD73 deficient osteoblasts. A: ALPase mRNA expression and activity of primary osteoblasts isolated from $cd73^{-/-}$ mice. Primary osteoblasts were isolated and cultured in mineralization medium for 6 days. ALPase mRNA expression and ALPase activity was determined as described in Materials and Methods Section. B: Mineral deposition by osteoblasts isolated from $cd73^{+/+}$ and $cd73^{-/-}$ mice. On days 9 and 12 of culture in mineralization medium, cells were fixed and stained with alizarin red S. The area of mineralization was measured photographically. Data are expressed as mean of area ± SE. [a]$P < 0.05$ compared with $cd73^{+/+}$ mice. C: The number of CFU-F and the percentage of CFU-OB in bone marrow cultures derived from $cd73^{+/+}$ and $cd73^{-/-}$ mice. CFU-F and CFU-OB assays were performed as described in Materials and Methods Section. Representative results from three experiments are shown. [Color figure can be seen in the online version of this article, available at http://wileyonlinelibrary.com/journal/jcp]

osteoblast differentiation but not in the development of osteoblast progenitors.

Osteoblast differentiation is accelerated in MC3T3-E1 cells over expressing CD73

To investigate the mechanism by which CD73 promotes osteoblast differentiation, we established MC3T3-E1 cells over expressing CD73 (MC/CD73) by transfecting with pHβ Apr-1-neo-cd73. Increased expression of CD73 in MC/CD73 is shown in Figure 4A. MC/CD73 cells exhibited normal cell shape (data not shown) and comparable proliferative ability (Fig. 4B). To examine the effects of CD73 over expression on differentiation, we cultured MC/CD73 cells in mineralization medium and assessed ALPase activity at weekly intervals. ALPase activity was significantly higher at days 7 and 14 compared with control transfectants (Fig. 4C). However, after

reaching peak activity on day 14, the ALPase activity of the MC/CD73 cells decreased more rapidly in the late stages of culture.

We next examined the expression of BSP and OC in MC/CD73 cells as differentiation markers of mature osteoblasts. As shown in Figure 4D, mRNA expression of BSP and OC was significantly higher in MC/CD73 cells compared with control transfectants, even when cells were cultured in normal culture medium, suggesting that over expression of CD73 promoted osteogenic potential. Elevated BSP and OC gene expression was further enhanced by cultivation in mineralization medium. Moreover, alizarin red S staining showed increased calcified nodule formation in MC/CD73 cells after 28 days of culture (Fig. 4E). These observations support the findings from primary osteoblast cultures that CD73 has a positive role in osteoblast differentiation and function.
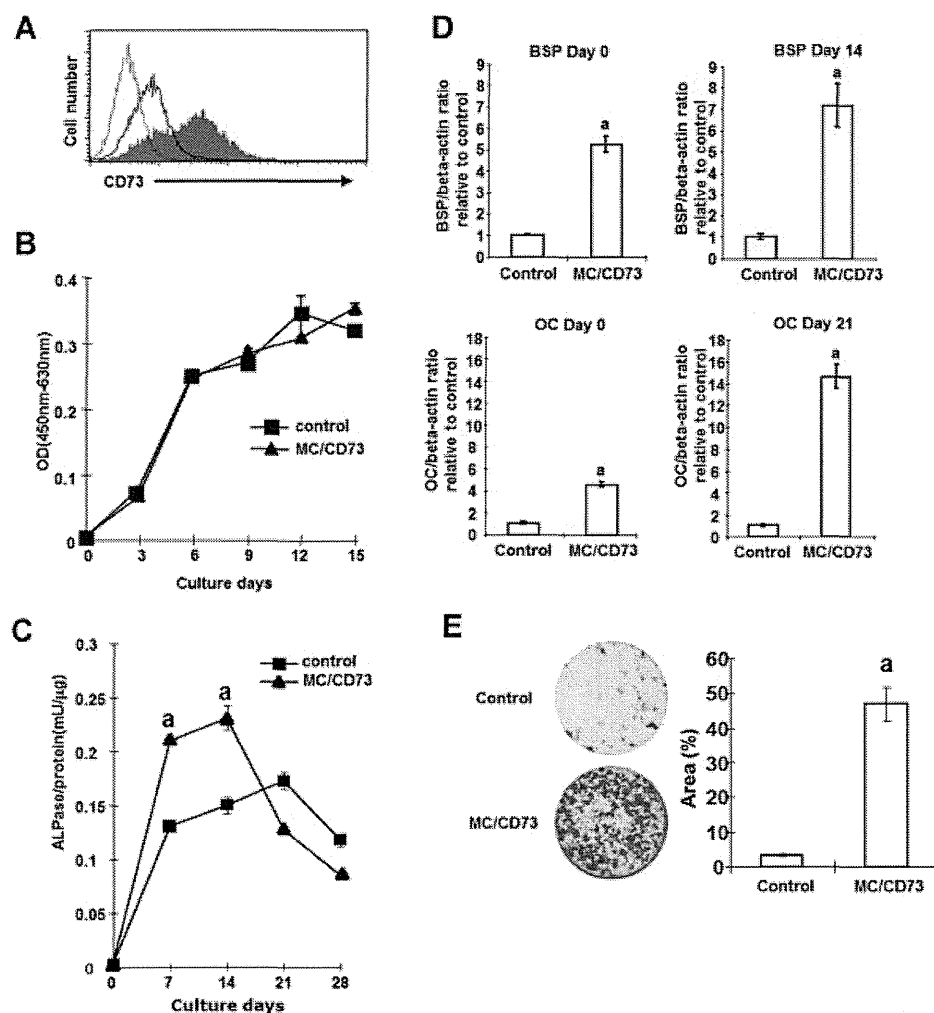
Fig. 4. Accelerated osteoblast differentiation in cd73-transfected MC3T3-E1 cells (MC/CD73). A: CD73 expression on MC/CD73 cells. CD73 expression on control cells is shown with the black line, and that on MC/CD73 cells is shown with the shaded histogram. Staining with an isotype control mAb is shown with the grey line. B: Proliferation of MC/CD73 and control cells. Cells were cultured in α-MEM supplemented with 10% FBS and OD450/630 was measured after reaction with WST-1 for 30 min on the indicated days. C: ALPase activities during differentiation in MC/CD73 and control cells. Cells were cultured with mineralization medium and ALPase activities were determined on the indicated days as described in the Materials and Methods Section. D: BSP and OC mRNA expression in MC/CD73 and control cells. Cells were cultured with or without mineralization medium for 14 or 21 days and BSP and OC mRNA levels were determined, respectively, by real-time PCR as described in Materials and Methods Section. E: Mineral deposition by MC/CD73 and control cells. On day 28 of culture in mineralization medium, cells were fixed and stained with alizarin red S. The area of mineralization was measured photographically. Data are expressed as mean of area $\pm$ SE. Representative results from more than three experiments are shown. [a]$P < 0.05$ compared with control cells. [Color figure can be seen in the online version of this article, available at http://wileyonlinelibrary.com/journal/jcp]

Adenosine receptor expression increases during osteoblastic differentiation of MC3T3-E1 cells

As CD73 is a major enzyme generating extracellular adenosine, we next evaluated AR expression on MC3T3-E1 cells. We performed RT-PCR analysis of each subtype of AR using RNAs isolated from the MC3T3-E1 cells cultured with mineralization medium. As shown in Figure 5A, expression of $A_{2A}AR$ and $A_{2B}AR$ were increased during culture in mineralization medium, and strong expression was observed in the later stages of osteoblast differentiation. Real-time PCR analysis confirmed the increase of $A_{2A}AR$ and $A_{2B}AR$ mRNA expression (Fig. 5B,C). In contrast, A_1AR and A_3AR mRNA were not detected throughout the culture by RT-PCR. To confirm the functional expression of $A_{2A}AR$ and $A_{2B}AR$ on MC3T3-E1 cells, cells were stimulated with exogenous adenosine in the presence or absence

of $A_{2A}AR$ and $A_{2B}AR$ antagonists (ZM241385 and MRS1754, respectively), and cAMP, the second messenger of both receptors, was measured. Significant increases of cAMP were observed by adding 100 μM adenosine to cells that had been cultured for 2 weeks in mineralization medium. This response to adenosine was suppressed in a dose-dependent manner by an $A_{2A}AR$ or $A_{2B}AR$ antagonist (Fig. 5D). These results demonstrated that differentiating osteoblasts express functional $A_{2A}AR$ and $A_{2B}AR$ and that their expression increases with differentiation.

CD73-generated adenosine stimulates osteoblasts via $A_{2B}AR$ signaling

Having demonstrated functional $A_{2A}AR$ and $A_{2B}AR$ on MC3T3-E1 cells, we next utilized ZM241385 and MRS1754 to determine if one or both of these receptors is involved in the